Resolving the Compartmentation and Function of C_4 Photosynthesis in the Single-Cell C_4 Species *Bienertia sinuspersici*[1][OA]

Sascha Offermann, Thomas W. Okita, and Gerald E. Edwards*

School of Biological Sciences (S.O., G.E.E.) and Institute of Biological Chemistry (T.W.O.), Washington State University, Pullman, Washington 99164

Bienertia sinuspersici is a land plant known to perform C_4 photosynthesis through the location of dimorphic chloroplasts in separate cytoplasmic domains within a single photosynthetic cell. A protocol was developed with isolated protoplasts to obtain peripheral chloroplasts (P-CP), a central compartment (CC), and chloroplasts from the CC (C-CP) to study the subcellular localization of photosynthetic functions. Analyses of these preparations established intracellular compartmentation of processes to support a NAD-malic enzyme (ME)-type C_4 cycle. Western-blot analyses indicated that the CC has Rubisco from the C_3 cycle, the C_4 decarboxylase NAD-ME, a mitochondrial isoform of aspartate aminotransferase, and photorespiratory markers, while the C-CP and P-CP have high levels of Rubisco and pyruvate, Pidikinase, respectively. Other enzymes for supporting a NAD-ME cycle via an aspartate-alanine shuttle, carbonic anhydrase, phospho*enol*pyruvate carboxylase, alanine, and an isoform of aspartate aminotransferase are localized in the cytosol. Functional characterization by photosynthetic oxygen evolution revealed that only the C-CP have a fully operational C_3 cycle, while both chloroplast types have the capacity to photoreduce 3-phosphoglycerate. The P-CP were enriched in a putative pyruvate transporter and showed light-dependent conversion of pyruvate to phospho*enol*pyruvate. There is a larger investment in chloroplasts in the central domain than in the peripheral domain (6-fold more chloroplasts and 4-fold more chlorophyll). The implications of this uneven distribution for the energetics of the C_4 and C_3 cycles are discussed. The results indicate that peripheral and central compartment chloroplasts in the single-cell C_4 species *B. sinuspersici* function analogous to mesophyll and bundle sheath chloroplasts of Kranz-type C_4 species.

Rubisco is the central CO_2 fixation enzyme in plants. It is a bifunctional enzyme, catalyzing the carboxylation as well as the oxygenation of ribulose-bisphosphate (RuBP) to 3-phosphoglycerate (3-PGA) and phosphoglycolate, respectively. While 3-PGA is subsequently utilized in the C_3 cycle to produce triose-phosphates, phosphoglycolate has no known metabolic use (Ogren, 1984) and needs to be detoxified by the plant. This process is known as photorespiration, which is not only energy consuming but also results in a net loss of previously fixed carbon and nitrogen. The rate of carboxylation versus oxygenation through Rubisco is directly related to the availability of CO_2 and the concentration of oxygen competing for the catalytic site of the enzyme. Since Rubisco is thought to have evolved under much higher levels of CO_2 than current atmospheric concentrations, it is believed that photorespiration was insignificant earlier in photosynthetic organisms. Under current atmospheric CO_2 levels, however, significant amounts (e.g. up to 25%) of previously fixed carbon may be lost through RuBP oxygenase activity under conditions that favor photorespiration, like high temperatures or water stress (Sage, 2004).

C_4 photosynthesis is an adaptation to suppress photorespiration and increase carbon gain. It acts as a CO_2 pump, increasing the CO_2 concentration around Rubisco, thereby effectively reducing its oxygenase activity. Accordingly, C_4 plants are some of the most productive plant species, having a higher water and nitrogen use efficiency through higher rates of photosynthesis at low intercellular levels of CO_2 and less investment in Rubisco protein in warmer climates than their C_3 counterparts. C_4 photosynthesis is usually associated with the so-called Kranz anatomy. Two specialized cell types, the mesophyll cells (MC) and bundle sheath cells (BSC), cooperate together in distinct anatomical configurations to concentrate CO_2 around Rubisco. MC and BSC show differences in the biochemistry of carbon fixation. For example, Rubisco accumulates in BSC chloroplasts, whereas phospho*enol*-pyruvate carboxylase (PEPC) and pyruvate, Pidikinase (PPDK) of the C_4 cycle accumulate in the cytosol and chloroplasts of MC, respectively. The differentiation of the two cell types is essential for the effective operation of C_4 photosynthesis (Hatch, 1987).

[1] This work was supported by the National Science Foundation (grant no. IBN–0641232).

* Corresponding author; e-mail edwardsg@wsu.edu.

The author responsible for distribution of materials integral to the findings presented in this article in accordance with the policy described in the Instructions for Authors (www.plantphysiol.org) is: Gerald E. Edwards (edwardsg@wsu.edu).

[OA] Open Access articles can be viewed online without a subscription.

www.plantphysiol.org/cgi/doi/10.1104/pp.110.170381

Depending on the biochemical subtype, which is based on the type of C_4 decarboxylase (NADP-malic enzyme [ME], NAD-ME, or phospho*enol*pyruvate carboxykinase [PEP-CK]) used to donate CO_2 to Rubisco, the two cell types also show significant specialization in the light reactions. Most noticeably, in NADP-ME species like sorghum (*Sorghum bicolor*) and maize (*Zea mays*), BSC chloroplasts are deficient in grana and have very limited capacity for whole-chain linear electron transport and, therefore, the generation of NADPH. In NAD-ME species, mitochondria are prominent in BSC, which is the site of C_4 acid decarboxylation. In all Kranz-type C_4 species, the cell wall is thought to contribute to diffusive resistance, limiting the leakage of CO_2 from the Rubisco-containing compartment (von Caemmerer and Furbank, 2003).

Recently, three species in family Chenopodiaceae have been shown to lack the requirement for Kranz anatomy in order to perform C_4 photosynthesis (Voznesenskaya et al., 2001, 2002, 2005; Chuong et al., 2006). Common to these so-called single-cell C_4 (SCC_4) species is that they do not possess MC and BSC but rather have two biochemically and morphologically different chloroplast types, which are spatially separated between two cytoplasmic domains within individual photosynthetic cells. In *Suaeda aralocaspica* (formerly *Borszczowia aralocaspica*), these two chloroplast types are arranged in elongated chlorenchyma cells, proximal and distal with respect to the internally located veins and water storage tissue. In contrast, *Bienertia cycloptera* and *Bienertia sinuspersici* show a more unique cell morphology. They have one chloroplast type distributed throughout the periphery (peripheral chloroplast [P-CP]) of the cell and the other chloroplast type (central compartment chloroplast [C-CP]) concentrated in a central compartment (CC) along with the mitochondria and peroxisomes, forming a ball-like structure in the center of the cell. The two compartments are spatially separated by a large vacuole and interconnected by a vacuole-spanning system of thin cytoplasmic channels (Voznesenskaya et al., 2005; Chuong et al., 2006).

It has been established from gas-exchange measurements, isotope discrimination analysis, and in situ immunolocalization of a few photosynthetic enzymes that *Bienertia* species perform C_4 photosynthesis within a single photosynthetic cell (Voznesenskaya et al., 2002, 2005; Chuong et al., 2006; Smith et al., 2009; Leisner et al., 2010). Accordingly, it has been proposed that in *B. sinuspersici*, P-CP might function analogous to MC and C-CP might function analogous to BSC in Kranz-type C_4 species; however, proof of function from studies at the subcellular level is lacking. The purpose of this study, therefore, was to develop a protocol for the isolation and purification of intact and functional dimorphic chloroplasts of *B. sinuspersici* for the analysis of enzyme composition as well as physiological function. It is demonstrated that P-CP and C-CP function analogous to MC and BSC chloroplasts in Kranz-type C_4 species with respect to carbon fixation. Interestingly, there is a large difference in the investment in chloroplasts (number and chlorophyll content) in the two compartments. The implications of this imbalance for the stoichiometry of the C_4 and C_3 cycles are discussed.

RESULTS

Isolation of Dimorphic Chloroplasts

Organelle distribution in the photosynthetic cells of *B. sinuspersici* is very different from that in other plant species (Fig. 1A). Chlorenchyma cells consist of P-CP located close to the cell wall within a thin layer of cytoplasm and C-CP that are located in a CC. Cytoplasmic channels spanning the central vacuole connect the compartments. Figure 1 shows a schematic of the isolation procedure (left) and micrographs illustrating the various steps (right). *B. sinuspersici* chlorenchyma cells can be isolated rapidly and easily due to the succulent nature of the leaves and the loose association of photosynthetic cells with each other. Vital staining with trypan blue dye showed that the majority of cells remained intact during the isolation procedure (Fig. 1B). Isolated cells were digested with cell wall-degrading enzymes, yielding protoplasts (Fig. 1C). A gentle method to break the protoplasts based on osmotic swelling was developed, which released the P-CP into the medium while the CC remained intact, as judged by visual inspection with a microscope (Fig. 1D). Then, differences in the density between the P-CP and the CC were used for their separation. Centrifugation at low speed (5 min, 40*g*) resulted in a pellet enriched in CC, which was further purified on a Percoll gradient (Fig. 1E) and a supernatant enriched in P-CP. The supernatant was subjected to two additional centrifugation steps to remove all remaining CC. Final purification of the P-CP was achieved by centrifuging through a 40% (v/v) Percoll cushion (Fig. 1H).

Developing a method to release functionally intact chloroplasts from the CC was especially challenging. It was previously shown that in *B. sinuspersici*, the cytoskeleton is tightly associated with the CC (Chuong et al., 2006). Since in vitro, high pH can inhibit the polymerization of tubulin (Galella and Smith, 1979), we tested whether a change in the buffer/pH of the medium could release chloroplasts from the CC, possibly by destabilizing the cytoskeleton (see Fig. 1 legend). Following treatments of the CC in HEPES buffer, pH 7.6, HEPES buffer, pH 8.0, or Tris buffer, pH 9.5 (Fig. 1I, tubes 1, 2, and 3 respectively), tubes were centrifuged (5 min, 40*g*), which will pellet intact CC but not individual chloroplasts. Figure 1I shows that incubation in HEPES buffer, pH 7.6, did not release significant amounts of chloroplasts, as judged by the almost clear supernatant (tube 1). Incubation in HEPES buffer, pH 8, released chloroplasts, as judged by the green supernatant (tube 2). The most efficient release of chloroplasts was obtained by incubation in Tris buffer, pH 9.5, where the supernatant was dark

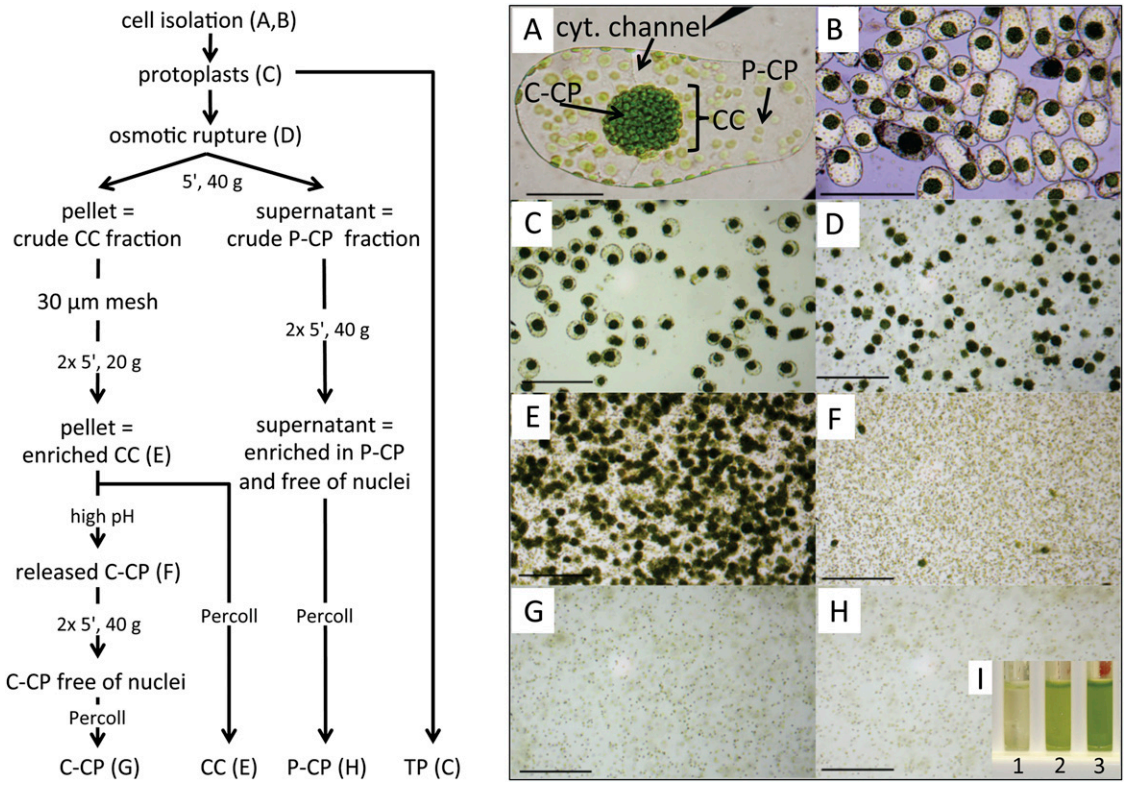

Figure 1. Method for isolation of the central compartment and the dimorphic chloroplasts from *B. sinuspersici* protoplasts. Left, Schematic overview of the isolation procedure. Right, micrographs illustrating the various steps in the procedure. Letters in parentheses in the scheme correspond to the micrographs on the right. A, Isolated chlorenchyma cell showing P-CP, C-CP, the CC, and the interconnecting cytoplasmic (cyt) channels. B, Vital stain of isolated chlorenchyma cells. C, Isolated protoplasts. D, Disrupted protoplasts. E, Purified CC. F, Chloroplasts that were released from the CC. G, Purified C-CP. H, Purified P-CP. I, Example of the effect of high pH on the stability of the CC. Isolated CC were incubated for 10 min on ice in HEPES buffer, pH 7.6 (tube 1), HEPES buffer, pH 8 (tube 2), or Tris buffer, pH 9.5 (tube 3). After incubation, the CC were pipetted gently up and down to determine if chloroplasts were released. Samples were centrifuged at low speed to pellet intact CC. The intensity of chlorophyll in the supernatant correlates with the efficiency of release of chloroplasts from the CC. Bar in A = 50 μm; bars in B to H = 200 μm.

green (tube 3). Figure 1F shows that the majority of chloroplasts were released from the CC and only a few CC remained intact after the Tris buffer, pH 9.5, treatment. The isolated chloroplasts were further purified by centrifugation through Percoll medium (Fig. 1G).

Intracellular Protein Distribution

Total protein extracts from the four isolated fractions, total protoplasts (TP), P-CP, CC, and C-CP (Fig. 1), were analyzed for the distribution of certain proteins by western-blot analysis. Equal amounts of protein were separated by SDS-PAGE, blotted onto nitrocellulose membranes, and visualized by Ponceau S staining (Fig. 2A). Qualitatively, there was some similarity in the band patterns for the different preparations, but it was apparent that certain protein bands were enriched or depleted in the four different preparations. Most noticeably, there was a strong band (arrow with one asterisk, presumably corresponding to Rubisco large subunit [RBCL]; see below) just above the 54-kD marker band, which was reduced in P-CP. Conversely, a second strong band (arrow with two asterisks, presumably corresponding to PPDK; see below) right below the 116-kD marker band was enriched in P-CP compared with the C-CP and CC. To test the effectiveness of the isolation procedure, the purification of organelles, and the distribution of proteins, six chloroplastic, three cytoplasmic, four mitochondrial, one peroxisomal, and one nuclear protein were analyzed by immunoblotting (Fig. 2B). The intensities of the bands were semiquantified by ImageJ software (Abramoff et al., 2004) and expressed as the percentage of the signal in the total protoplast preparation. Throughout, Rubisco and PPDK served as markers for the two chloroplast types, since they have been shown to accumulate differentially in P-CP and C-CP from in situ immunolocalization studies in the related SCC_4 species *B. cycloptera* (Voznesenskaya et al., 2002, 2005). The immunoreactive band for RBCL was stronger in C-CP (approximately 3.5 times) and CC (approximately three times) than in P-CP. The small subunit of Rubisco (RBCS) was more abundant

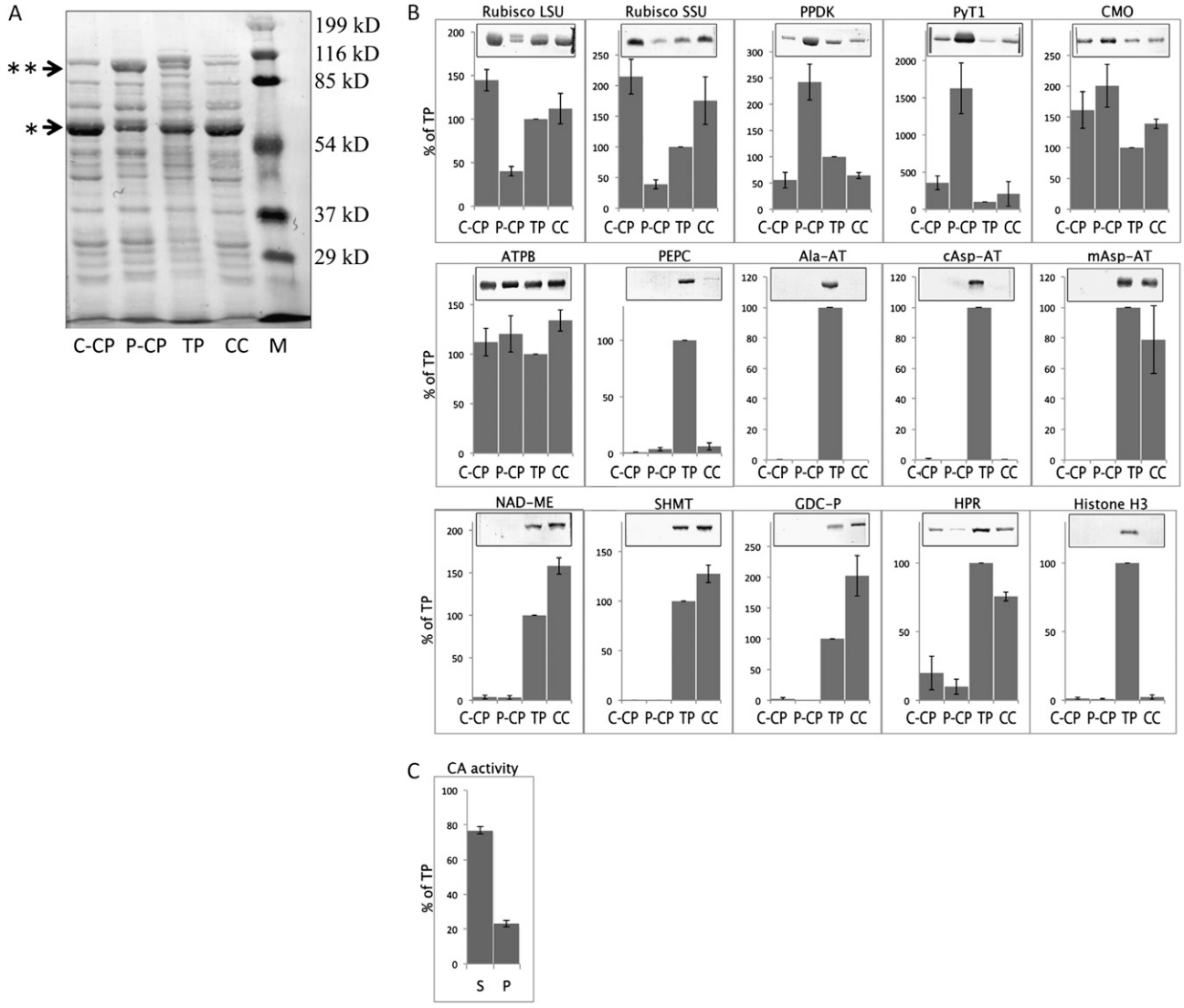

Figure 2. Protein distribution in isolated chloroplasts. C-CP, P-CP, TP, and CC were isolated as described in Figure 1 and subjected to western-blot analysis. Equal amounts of total protein extract from the four different preparations were resolved on 15% (v/v; Rubisco small subunit [SSU] and histone H3) or 10% (v/v; all other proteins) polyacrylamide gels. Five micrograms of protein was loaded per lane for analysis of the Rubisco large subunit (LSU) and small subunit, PPDK, and PEPC, and 20 μg was loaded for all other proteins. A, Ponceau S stain of proteins (20 μg) resolved by SDS-PAGE and blotted onto nitrocellulose membranes. Asterisks indicate bands enriched in C-CP (*) and P-CP (**). B, Western blots were obtained using antibodies against Rubisco large subunit and small subunit, PPDK, PyT1, choline monooxygenase (CMO), β-subunit of ATP-synthase (ATPB), PEPC, Ala-AT, cAsp-AT, mAsp-AT, NAD-ME, SHMT, GDC-P, HPR, and histone H3. The quantification of the immunoreactive bands was expressed as a percentage of the amount in the total protoplast extract. C, Localization of CA. Protoplasts were isolated as described in "Materials and Methods," and the chloroplasts containing pellet (P) were separated from the supernatant (S) by centrifugation. CA activity was measured titermetrically and was expressed as the percentage of the activity in total protoplast extracts. Values represent averages of three independent experiments for Ala-AT, cAsp-At, and mAsp-AT and four independent experiments for all other analyses. Error bars represent SE. M, Molecular mass standard.

in CC and C-CP (approximately four to five times) than in P-CP. The immunoreactive band for PPDK was stronger in P-CP (approximately four to five times) than in C-CP and CC. Comparing the immunoblots with the total protein stain pattern in Figure 2A suggests that the observed differentially accumulating protein bands are indeed RBCL (single asterisk, approximately 55 kD) and PPDK (double asterisk, approximately 98 kD), respectively. Besides PPDK, we also found the putative C_4-specific Na^+-dependent chloroplastic pyruvate transporter (PyT1; Furomoto et al., 2009) to be about 4- to 5-fold enriched in P-CP over CC and C-CP. In contrast, choline monoxygenase, a stromal protein involved in the synthesis of Gly

betaine, accumulated to similar levels in the two chloroplast types, as did the β-subunit of ATP synthase. PEPC was apparently not located in organelles, since a strong signal was obtained from the total protoplast preparation but there was very low detection in the two chloroplasts types and in the CC. A similar result was observed with antibodies directed against alanine aminotransferase (Ala-AT) and the cytosolic isoform of aspartate aminotransferase (cAsp-AT), indicating that they are located in the cytosol. Putative markers for mitochondria, the mitochondrial isoform of aspartate aminotransferase (mAsp-AT), the C_4 decarboxylation enzyme NAD-ME, serine hydroxymethyltransferase (SHMT), and the P-subunit of Gly decarboxylase (GDC-P) of the photorespiratory pathway, were abundant in the CC and in the TP and essentially undetectable in P-CP and C-CP. This demonstrates that these enzymes are localized within the CC but not in the chloroplasts. Hydroxypyruvate reductase (HPR1), a putative marker for peroxisomes (Timm et al., 2008), showed the highest band intensity in the total protoplast preparation, followed by a strong signal in CC and a low but clearly detectable signal in C-CP and P-CP. Finally, histone H3 served as a marker for nuclear contamination and was only detectable in the total protoplast preparation.

Due to the lack of a specific antibody, we measured partitioning of carbonic anhydrase (CA) enzymatically. The activity of CA in protoplast extracts in Wilbur-Anderson units (Wilbur and Anderson, 1948) was 4.2 ± 0.43 units mg^{-1} total protein. Protoplasts were disrupted and immediately fractionated into a supernatant and a chloroplast-containing pellet; approximately 77% of the total CA activity was in the supernatant and only approximately 23% activity was associated with the pellet (Fig. 2C). To ensure integrity of the chloroplasts, aliquots of the preparations were simultaneously analyzed for their contents of the soluble stromal proteins PPDK and RBCL; 72% ± 11% of PPDK and 86% ± 13% of RBCL were found in the pellet fraction, indicating that the majority of chloroplasts remained intact during the procedure. This indicates that the major fraction of CA in the supernatant is cytosolic and not due to the loss of a chloroplast form by organelle breakage.

Photosynthetic Oxygen Evolution

To analyze chloroplast functions, we measured photosynthetic oxygen evolution (POE) in the two types of purified chloroplasts, the CC and the isolated photosynthetic cells with additions of different substrates. Intact cells were used for comparison with isolated chloroplasts, since protoplasts tend to break easily in the oxygen electrode chamber due to mechanical stress from the magnetic stirrer. Figure 3A shows the rates of POE with isolated cells (taken from the maximum slope of oxygen evolution following induction by illumination at different light intensities) at 25°C and in the presence of 10 mM bicarbonate. The rates of POE increased with increasing light intensity up to full sunlight (photosynthetic photon flux density [PPFD] of 2,000 μmol quanta $m^{-2} s^{-1}$), reaching a maximum of approximately 100 μmol oxygen mg^{-1} chlorophyll h^{-1}. A PPFD of 1,000 was used in subsequent experiments to minimize the potential for photoinhibition with the isolated chloroplasts. Since *B. sinuspersici* is adapted to warm climates (Akhani et al., 2005), the response of POE to temperature (maximum rates and stability during assay) was analyzed with isolated cells, in comparison with purified chloroplasts. Figure 3B shows the response with isolated cells at 1,000 PPFD and in the presence of 10 mM bicarbonate. Between 25°C and 40°C, POE increased continuously and reached its maximum at 40°C. POE was slightly reduced at 45°C and completely inhibited at 50°C. Although the highest rates for isolated cells were observed at 40°C, photosynthesis in isolated chloroplasts at the same temperature was low and unstable. Further experimentation demonstrated that more reproducible results could be obtained at lower temperatures (data not shown). Therefore, the remaining experiments on POE were performed at 25°C and 1,000 PPFD.

Bicarbonate dependence of POE was measured in isolated cells under varying concentrations of HCO_3^- (Fig. 3C). Using 10 mM bicarbonate as the CO_2 source in the reaction medium, high POE was measured (approximately 80 μmol oxygen mg^{-1} chlorophyll h^{-1}). Without the addition of bicarbonate, isolated cells can still evolve oxygen at a relatively high rate (approximately 25 μmol oxygen mg^{-1} chlorophyll h^{-1}). When the reaction mixture was treated with gaseous nitrogen prior to measurement in order to remove CO_2 completely from the medium, POE was reduced to a very low level (less than 5 μmol oxygen mg^{-1} chlorophyll h^{-1}).

Next, POE was measured with a variety of substrates to study the functional differentiation of the two chloroplast types in using reductive power for carbon assimilation. Figure 3D illustrates CO_2-dependent POE in the presence of 10 mM bicarbonate in isolated total intact cells (TC), C-CP, P-CP, and CC. Results from all experiments were calculated on a chlorophyll basis (using 12.5 μg of chlorophyll per 0.5 mL of reaction medium) at 1,000 PPFD and 25°C. Cells or isolated chloroplasts were transferred to the oxygen electrode reaction chamber and incubated for 1 min in the dark. Light was turned on and POE was recorded over a period of 20 min (10 min for C-CP). Isolated whole cells began to evolve oxygen almost immediately after illumination and continued with a high linear rate for about 8 min. After this time period, the rate of POE decreased and then reached a constant low rate approximately 15 min after illumination. In contrast, POE in C-CP, P-CP, and CC increased slowly during the first 4 min of illumination, followed by high linear POE rates for C-CP and CC (lasting for at least 6–8 min). The maximum POE rates for C-CP and CC (40 μmol oxygen mg^{-1} chlorophyll h^{-1}) were half the

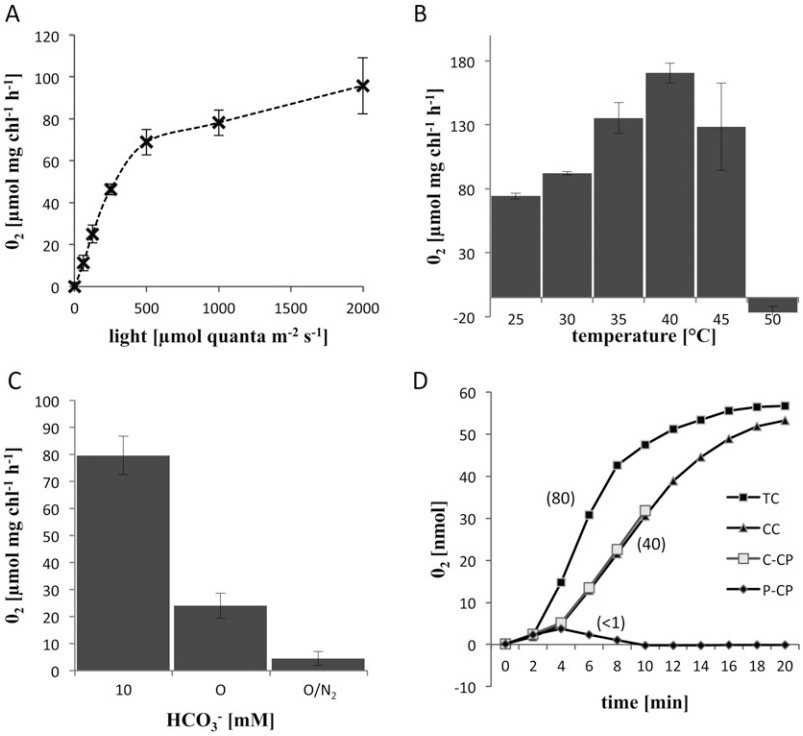

Figure 3. Photosynthetic oxygen evolution in isolated chloroplasts, the CC, and TC. A to C, Light, temperature, and CO_2 responses of POE in isolated *B. sinuspersici* cells. Values represent averages of three independent experiments, and error bars represent SE. D, Example of CO_2-dependent POE in P-CP, C-CP, the CC, and TC. POE was recorded for a time period of 20 min, except for C-CP (10 min). Numbers in parentheses represent maximum rates expressed as μmol oxygen mg^{-1} chlorophyll h^{-1}. Average values and SE of four independent replicates for this experiment are found in Table I. Bicarbonate (10 mM) was included as an inorganic carbon source in all experiments except for C, where inorganic carbon concentration is indicated in the figure. 0/N_2, No addition of inorganic carbon and additional treatment with gaseous nitrogen to remove residual CO_2 from the reaction, as explained in the text.

maximum rate of TC (80 μmol oxygen mg^{-1} chlorophyll h^{-1}). In contrast, P-CP did not show significant POE in the presence of CO_2; after illumination, there was a low initial rate (less than 1 μmol oxygen mg^{-1} chlorophyll h^{-1}), which was followed by a low rate of oxygen consumption in the light.

Table I summarizes the average maximum POE rates with different substrates from four independent replicates with SE values in parentheses. As noted above, only C-CP, CC, and TC showed CO_2-dependent POE. Without the addition of inorganic carbon to the reaction medium ($-HCO_3^-$), only TC evolved oxygen (the rate at normal atmospheric conditions was approximately 3.5 times lower than in the presence of HCO_3^-). Oxygen evolution in the presence of CO_2 was light dependent. To test the specificity of the CO_2-dependent oxygen evolution for the C_3 cycle, we measured POE in the CC in the presence of glyceraldehyde (GA), a specific C_3 cycle inhibitor (Stokes and Walker, 1972). No significant POE could be observed in GA-treated CC despite the presence of HCO_3^-.

When testing 3-PGA (measured in the presence of N_2 to remove residual CO_2 from the medium, as described previously) as a possible substrate for light-dependent oxygen evolution associated with the reductive phase of the C_3 cycle, both the C-CP and CC showed higher POE rates (82 and 53 μmol oxygen mg^{-1} chlorophyll h^{-1}, respectively) compared with those with HCO_3^- (40 and 42 μmol oxygen mg^{-1} chlorophyll h^{-1}, respectively). The P-CP also showed high rates of POE with 3-PGA (69 μmol oxygen mg^{-1} chlorophyll h^{-1}). 3-PGA-dependent oxygen evolution was low in TC.

We further tested whether oxaloacetate (OAA) could serve as a substrate for photosynthetic oxygen evolution in P-CP, which could occur if it were taken

Table I. *Substrate-dependent photosynthetic oxygen evolution in B. sinuspersici cells and subcellular compartments*

Different substrates (HCO_3^-, PGA, OAA, Pyr, and pBQ) were tested for their ability to induce oxygen evolution in the two different chloroplasts types, the CC, and isolated TC. Control experiments without light and with the C_3-cycle inhibitor GA are shown as well. Values are averages of the maximum rates of four independent experiments and are expressed as μmol oxygen mg^{-1} chlorophyll h^{-1}. Numbers in parentheses represent SE. Oxygen evolution rates less than 1 μmol oxygen mg^{-1} chlorophyll h^{-1} were considered to be insignificant. The last column shows intactness (%) measured by ferricyanide (FC)-dependent photosynthetic oxygen evolution determined from isolated intact and osmotically shocked chloroplasts. n.d., Not determined.

Substrate	$+HCO_3^-$	$-HCO_3^-$	−Light	+GA	+3-PGA	+OAA	+Pyr	+OAA,+Pyr	pBQ	FC
TC	83 (7.2)	24.9 (2.0)	<1	n.d.	<1	n.d.	n.d.	n.d.	95 (4.1)	n.d.
CC	42 (3.1)	<1	<1	<1	53 (4.3)	n.d.	n.d.	n.d.	90 (11.5)	74 (4.9)
C-CP	40 (1.8)	<1	<1	n.d.	82 (11.0)	n.d.	n.d.	n.d.	n.d.	77 (7.8)
P-CP	1 (0.4)	<1	<1	n.d.	69 (3.4)	<1	<1	<1	111 (16.1)	86 (9.2)

up and reduced to malate (MA) via NADP-malate dehydrogenase (NADP-MDH). The effect of OAA in combination with pyruvate (Pyr) was also tested, since Pyr can stimulate OAA-dependent oxygen evolution through the utilization of ATP during the conversion of Pyr to phospho*enol*pyruvate (PEP) through PPDK, which prevents excessive buildup of the proton motive force (Huber and Edwards, 1975). No POE was observed in P-CP, with the addition of OAA and Pyr, OAA alone, or Pyr alone.

To test for PSII capacity in the two chloroplast types, POE was measured in the presence of the artificial Hill oxidant parabenzoquinone (pBQ). It accepts electrons from PSII, thereby providing a measure of PSII activity when bypassing whole-chain electron flow (Cho et al., 1966). pBQ-dependent POE rates were high and similar in P-CP, TC, and CC, indicating that both chloroplast types have a comparable PSII capacity to evolve oxygen. Finally, intactness of the preparations was measured at the end of the experiments on each replicate with the ferricyanide test (see "Materials and Methods"). On average, intactness was 74% to 86% after storage of the chloroplasts on ice for more than 4 h.

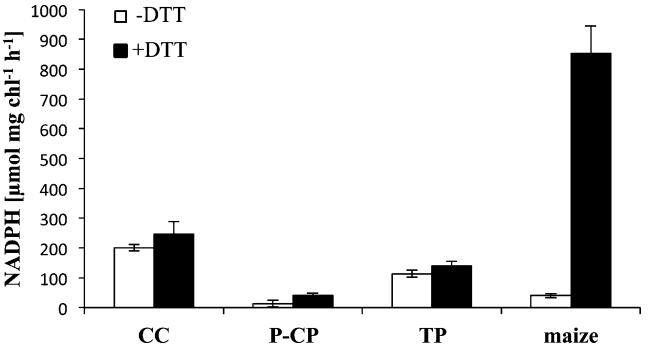

Figure 4. NADP-MDH assay. CC, P-CP, and TP were prepared as described previously and lysed in NADP-MDH buffer (see "Materials and Methods"). Maize leaf extract was prepared by grinding whole maize leaves in NADP-MDH assay buffer and filtering the extract through a 30-μm nylon mesh. Chlorophyll was determined, and chloroplasts corresponding to 10 μg of total chlorophyll were used from each preparation for each measurement. Samples were preincubated for 15 min at room temperature in NADP-MDH buffer either without (white bars) or with (black bars) 25 mM DTT. NADP-MDH was assayed spectrophotometrically by measuring the oxidation of NADPH at 340 nm and 35°C. Reactions were started after 2 min by adding 3 mM OAA to the reaction buffer. Values represent averages of three independent experiments, and error bars represent SE.

NADP-MDH Activity

Since oxygen evolution measurements indicated that P-CP do not reduce OAA to MA (Table I), preparations were enzymatically assayed for NADP-MDH activity by monitoring the oxidation of NADPH to $NADP^+$ with OAA as substrate. Activity was measured in extracts of CC, P-CP, and TP in either the presence (black bars) or absence (white bars) of dithiothreitol (DTT; Fig. 4). DTT was used to test the specificity of the reaction for chloroplastic NADP-MDH, which is redox activated (Johnson and Hatch, 1970). Maize leaf extracts were used as a positive control, since maize is known to reduce OAA to MA in the chloroplasts of MC by NADP-MDH as part of the C_4 carbon shuttle (Hatch and Osmond, 1976). NADPH-oxidizing activities were observed in extracts of CC and TP (approximately 250 and approximately 150 μmol NADPH mg^{-1} chlorophyll h^{-1}, respectively). P-CP showed very low rates (less than 50 μmol NADPH mg^{-1} chlorophyll h^{-1}), while NADP-MDH activity in maize was approximately 850 μmol NADPH mg^{-1} chlorophyll h^{-1}. In maize leaf extracts, NADP-MDH activity was reduced approximately 20-fold in the absence of DTT (from approximately 850 to less than approximately 40 μmol NADPH mg^{-1} chlorophyll h^{-1}). In contrast, in the tested preparations of *B. sinuspersici*, there was no significant reduction in NADPH-oxidizing activity in the absence of DTT.

PEP Formation by Isolated Chloroplasts

One of the main functions of mesophyll chloroplasts in C_4 photosynthesis is to regenerate the primary CO_2 acceptor PEP from Pyr, which is catalyzed by the enzyme PPDK. The reaction cannot be analyzed directly by measuring POE, since the ATP-dependent formation of PEP does not require reductive power. In order to determine whether the P-CP in *B. sinuspersici* function analogously to mesophyll chloroplasts in Kranz-type C_4 species, we measured PEP synthesis in isolated P-CP versus CC. P-CP were illuminated for the indicated time periods in the presence of Pyr (Fig. 5A). Chloroplasts were removed by centrifugation, and the supernatants were analyzed enzymatically for their PEP content by coupling to PEPC and MA dehydrogenase (see "Materials and Methods"). Without illumination, the amount of PEP detectable in the supernatant at zero time was very low (less than 5 nmol). Upon illumination of P-CP in the presence of Pyr, PEP formation continuously increased over the measured time period of 40 min. Next, the ability of P-CP versus the CC to form PEP was compared (Fig. 5B). Isolated preparations were incubated for 10 min in the light and in the presence of Pyr. The rate of PEP formation was about five times lower in CC (30 μmol PEP mg^{-1} chlorophyll h^{-1}) than in P-CP (150 μmol PEP mg^{-1} chlorophyll h^{-1}). Control experiments without light (P-CP −light) or without Pyr (P-CP −Pyr) showed only very low levels of PEP formation (10 and 5 μmol PEP mg^{-1} chlorophyll h^{-1}, respectively). NADH oxidation was barely detectable (less than 5 μmol PEP mg^{-1} chlorophyll h^{-1}) in P-CP that were illuminated for 10 min in the presence of Pyr without the addition of the coupling enzymes, PEPC, and NADH-MDH.

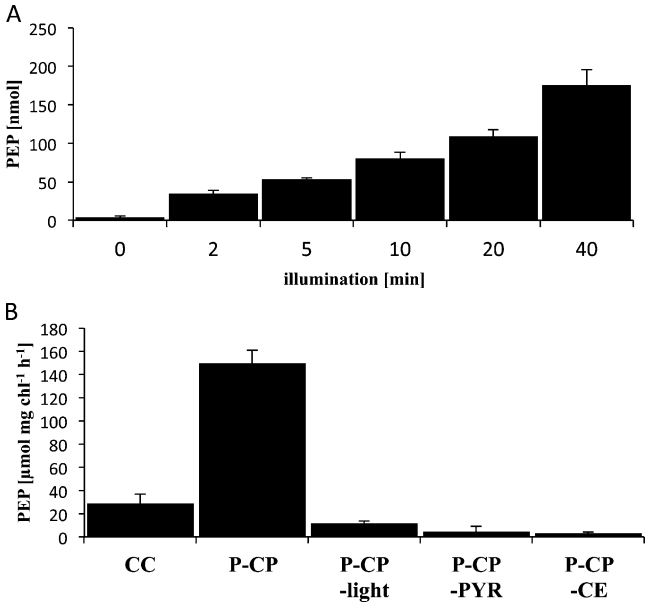

Figure 5. PEP formation by isolated chloroplasts. A, P-CP were isolated as described previously, and amounts corresponding to 20 μg of total chlorophyll were resuspended in PEP assay buffer containing Pyr (see "Materials and Methods"). Chloroplasts were illuminated with 1,000 μmol quanta m^{-2} s^{-1} at 25°C under constant stirring. Aliquots of the reaction medium (corresponding to 2 μg of chlorophyll) were removed from the illumination chamber at the indicated time points, and chloroplasts were immediately pelleted by centrifugation. NADH was added to the clarified supernatant, and PEP formation was assayed spectrophotometrically by monitoring the oxidation of NADH at 340 nm. The reaction was initiated by adding the coupling enzymes (30 units of purified PEPC and 10 units of purified NADH-MDH). Values represent averages of three independent experiments, and error bars represent SE. B, Substrate- and light-specific PEP formation. Assay conditions were as described in A. CC and P-CP were illuminated in the presence of Pyr for 10 min, and PEP formation was measured by monitoring NADH oxidation (purified C-CP were not analyzed to avoid possible loss of function during further processing of the CC). P-CP were also tested in the presence of Pyr without light (P-CP –light), in the light without Pyr (P-CP –Pyr), and without the addition of the coupling enzymes (CE) to the reaction mixture (P-CP –CE). Values represent averages of three independent experiments, and error bars lines represent SE.

Chloroplast Distribution and Chlorophyll and Protein Contents

To determine the investment in development of the two chloroplast types within *B. sinuspersici* chlorenchyma cells, the number of P-CP and C-CP per cell and the respective amounts of chlorophyll and protein were determined. The dense packing of organelles in the CC did not allow for direct counting of individual chloroplasts (Fig. 1A). Therefore, isolated protoplasts were gently broken by pressing on the coverslip of a microscope glass slide. This allowed the chloroplasts, which were released from individual protoplasts, to be counted and the two types of chloroplasts to be distinguished (Fig. 6). Individual broken protoplasts were analyzed when the CC was sufficiently dispersed to allow counting and when the P-CP were in close proximity, so that an unambiguous identification was ensured. The surrounding area was examined for any scattered chloroplasts and to ensure that there were no other broken protoplasts nearby. Chloroplasts were counted manually from photographs and marked with the aid of image-manipulation software (triangles and circles) to avoid redundant counting (Fig. 6A). On average, the central compartment had about six times more chloroplasts (355 ± 25.4) than the peripheral compartment (62 ± 9.1; Table II). We could verify the number of P-CP independently by analyzing reconstructed three-dimensional models (Z-scans) of *B. sinuspersici* cells using confocal microscopy and autofluorescence of the chloroplasts (data not shown); but again, the dense packing of the chloroplasts within the CC did not allow counting the number of C-CP per cell

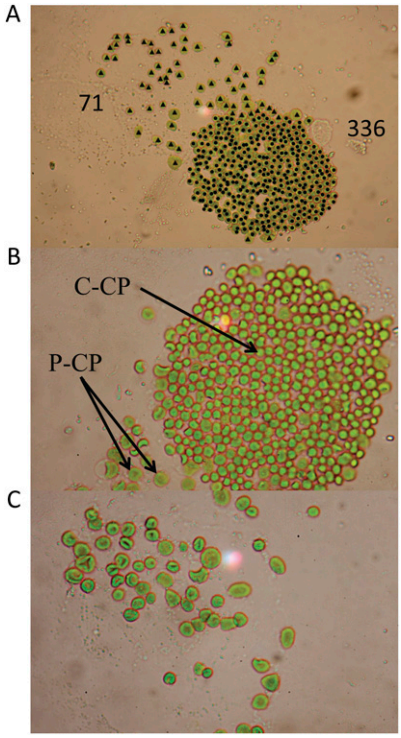

Figure 6. Distribution and appearance of peripheral and central chloroplasts within individual chlorenchyma cells. Protoplasts were prepared as described in "Materials and Methods." Diluted aliquots of the preparation were spotted onto the microscope slide, and a coverslip was gently applied. The pressure from the coverslip disrupted the protoplasts so that the individual chloroplasts came to rest in the same focal plane and the CC became dispersed, so that individual chloroplasts become visible. A, Example of a micrograph used to quantify the numbers of P-CP and C-CP within an individual cell. Chloroplasts were counted from micrographs, and individual P-CP and C-CP were marked with triangles and circles, respectively, to avoid redundant counting. Numbers for this example are shown. Results are summarized in Table II. B, Magnification of a dispersed CC. Individual C-CP are visible and can be distinguished from P-CP by their size and shape. C, Magnification of P-CP. P-CP are larger than C-CP and have a distinguishing doughnut-like shape. Magnification in A, 100×; in B and C, 400×.

Table II. *Chloroplast distribution and visible surface area*

Numbers of individual P-CP and C-CP were determined microscopically as described in Figure 6. Determination of the visible surface area per chloroplast was performed by outlining the chloroplast areas manually with the aid of ImageJ software. Values are averages of 15 independent counts ± SE.

Parameter	P-CP	C-CP	C-CP/P-CP	P-CP + C-CP
No. of chloroplasts per cell	62± 9.1	355± 25.4	5.7± 0.93	417 ± 26.98[a]
Visible surface area per chloroplast (10^3 pixels)	6.51± 0.41	3.27± 0.09	0.5± 0.034	—

[a]Calculated by summing values from P-CP and C-CP.
—, Not determined.

by this method. Visually, P-CP appeared larger and had a more doughnut-like shape, while the C-CP were smaller and more round (Fig. 6, B and C). Quantification showed that the visible surface area of a P-CP (6.51×10^3 pixels) was twice as large as the visible surface area of a C-CP (3.27×10^3 pixels; Table II). The chlorophyll and protein contents, as well as chlorophyll *a*/*b* ratios, were determined from isolated chloroplasts and protoplasts (Table III). Aliquots of each preparation were counted with a hematocytometer, which then allowed the calculation of chlorophyll and protein content per chloroplast and per protoplast. The total chlorophyll content per protoplast was, on average, 431 pg. The P-CP contained approximately 30% more chlorophyll per chloroplast (0.89 pg) than the C-CP (0.63 pg). The chlorophyll *a*/*b* ratio was similar in TP, P-CP, and C-CP (5.3, 4.5, and 4.8, respectively). The amount of total protein per protoplast was approximately 6.9 ng, and the amount of protein in P-CP and C-CP was similar (8.8 and 9.5 pg per chloroplast, respectively).

The amounts of chlorophyll and total protein invested in the two types of chloroplasts within a photosynthetic cell were calculated. For each chloroplast type, the chlorophyll and protein contents per chloroplast (as determined from isolated chloroplasts) were multiplied by the average chloroplast number per cell (determined from counting with the light microscope; Table IV). The *B. sinuspersici* chlorenchyma cells had about four times more chlorophyll (224 versus 55 pg) and six times more total protein (3,390 versus 548 pg) invested in the C-CP than in the P-CP. About 57% of the total protein per cell was located within the two chloroplast types, with 49% within the C-CP and 7.9% within the P-CP. Finally, the chloroplasts of the CC had a combined visible surface area that was about three times larger ($1{,}161 \pm 89 \times 10^3$ pixels) than the P-CP ($404 \pm 65 \times 10^3$ pixels).

DISCUSSION

In this study, evidence is provided on the intracellular compartmentation of functions to support a NAD-ME-type C_4 cycle in the SCC_4 species *B. sinuspersici*. It was shown that the two different chloroplast types, as well as the central compartment, can be isolated and separated with a high degree of purity when considering cross-contamination and contamination with other cellular components. Our analyses show that P-CP and C-CP function analogous to MC and BSC chloroplasts in Kranz-type NAD-ME C_4 species with respect to primary carbon metabolism. This is supported by the distribution pattern of marker enzymes for the C_4 and C_3 cycles as well as by characterization of light-dependent functions of the chloroplasts.

Development of an Isolation Protocol to Obtain Pure, Intact Chloroplasts

Much of our current understanding of C_4 photosynthesis was obtained when effective isolation procedures for the MC and BSC types of Kranz-type C_4 species were developed (for a review of the methodology for separating MC and BSC and the history of Kranz C_4 research, see Edwards et al., 2001). Due to the fact that C_4 photosynthesis occurs in *B. sinuspersici* within a single cell that contains two morphologically and biochemically distinct chloroplast types, the development of a completely new isolation procedure for the characterization of the two chloroplast types was required. During establishment of the isolation procedure, it was apparent that, after rupture of the protoplasts, the CC remains intact (Fig. 1D). This raised the question of what keeps the CC together structurally. Recently, it has been shown that the cytoskeleton, and most notably the microtubules, form a cage around the

Table III. *Chlorophyll and protein contents*

P-CP, C-CP, and TP were isolated as described previously, and chlorophyll and total protein were determined as described in "Materials and Methods." Particles in diluted aliquots of each preparation were counted in a hematocytometer to allow calculation of chlorophyll and protein per chloroplast or cell. Values are averages of four independent experiments ± SE.

Parameter	Per P-CP	Per C-CP	Per TP	C-CP/P-CP
Chlorophyll content (pg)	0.89 ± 0.05	0.63 ± 0.03	430.80 ± 30.7	0.71 ± 0.05
Chlorophyll *a*/*b*	4.5 ± 0.39	4.8 ± 0.41	5.3 ± 0.61	1.1 ± 0.13
Protein content (pg)	8.83 ± 1.05	9.54 ± 0.65	6,936 ± 750	1.1 ± 0.15

Table IV. *Calculated chlorophyll and protein distribution on a per cell basis*

Numbers for the two different chloroplast types from Table II were multiplied with the chloroplast and protein content per chloroplast from Table III. Since the data were from two nonrelated experiments, new SE values were calculated by applying the laws of error propagation.

Parameter	P-CP	C-CP	C-CP/P-CP	P-CP + C-CP
Chlorophyll per cell (pg)	55.2 ± 8.67[a]	223.7 ± 16.94[a]	4.1 ± 0.71	278.9 ± 19.03[b]
Total protein per cell (pg)	547.5 ± 103.4[a]	3,387 ± 334.6[a]	6.2 ± 1.32	3,935 ± 350.2[b]
Fraction of total cell protein (%)	7.9 ± 0.87	49 ± 0.72	6.2 ± 0.69	56.9 ± 1.13[b]
Fraction of total chloroplast protein (%)	13.9 ± 2.90	86.1 ± 11.44	6.2 ± 1.53	—
Visible chloroplast surface area/cell (10^3 pixels)	403.62 ± 64.5[a]	1,160.9 ± 88.99[a]	2.9 ± 0.51	—

[a]Calculated by multiplying the number of chloroplasts by the chlorophyll/protein content per chloroplast. [b]Calculated by summing values from P-CP and C-CP.

—, Not determined.

CC that is important for structural integrity. Nevertheless, it was speculated that in vivo, the tonoplast membrane (mediated by the pressure of the vacuole) might be partially responsible for maintaining the structure of the CC (Chuong et al., 2006; Park et al., 2009). Our study shows that, even after disrupting the cell and thereby disrupting the vacuole, the CC remains undamaged and is very resistant to mechanical force. This suggests that the structure of the CC is not primarily dependent on the vacuole pressure but is sustained by the cytoskeleton. No evidence was found for a membrane around isolated CC by electron microscopy (J. Park and G.E. Edwards, unpublished data). Isolation of C-CP from CC, which apparently occurs by disrupting the cytoskeleton, was achieved by incubation in a high-pH buffer (Fig. 1, F and I). Inhibition of polymerization of tubulin by high pH in vitro has been attributed to sensitivity of the microtubule-associated protein fraction rather than the tubulin proteins themselves (Galella and Smith, 1979). The release of chloroplasts from the CC at high pH might be attributed to destabilization at the interface between chloroplasts and the cytoskeleton (e.g. on proteins that anchor the chloroplasts to the cytoskeleton) rather than directly on the cytoskeleton itself. The existence of such proteins has been described in interactions between chloroplasts and the actin cytoskeleton, mediated by CHUP1 in Arabidopsis (*Arabidopsis thaliana*; Oikawa et al., 2003).

Since the main purpose of this study was to analyze the physiological functions of the two different chloroplast types, there was careful assessment of the quality of the isolated preparations. The Percoll utilized in the final step of the chloroplast isolation procedure separates intact from broken chloroplasts, due to differences in their buoyant density. In these preparations, approximately 50% of all chloroplasts (regardless of the type) were partitioned into the denser Percoll layer, indicative of a yield of approximately 50% intact chloroplasts. Additionally, the ferricyanide test (Table I) shows a high degree of intactness of the Percoll-purified chloroplasts, even after storage of the chloroplasts for several hours. It is important to note, however, that this test cannot differentiate between fully intact and functional chloroplasts and chloroplasts that were broken and resealed. Therefore, the ferricyanide test may overestimate the degree of intactness (Lilley et al., 1975). The ultimate criterion for chloroplast integrity is testing for physiological function. Isolated C-CP and CC had substantial rates of oxygen evolution with CO_2 as a substrate, indicating a fully operational C_3 cycle (Fig. 3D). Since the C_3 cycle requires the coordinated operation of 11 enzymes and function of the phosphate transporter, we concluded that the isolated C-CP and CC retain photosynthetic enzymes. No CO_2-dependent oxygen evolution was observed with isolated P-CP; however, they were capable of 3-PGA-dependent POE (Fig. 3D; Table I). This reaction does not require a fully functional C_3 cycle but only the reductive phase, consisting of phosphorylation and subsequent reduction of 3-PGA to glyceraldehyde-3-phosphate by glyceraldehyde phosphate dehydrogenase. This indicates that the chloroplasts are intact, since broken chloroplasts (thylakoids) would not retain these enzymes or the adenylates and NADPH needed for function of the reductive phase. Finally, isolated P-CP were capable of light-dependent conversion of Pyr to PEP (Fig. 5A). This involves the uptake and phosphorylation of Pyr to PEP, the export of PEP out of the chloroplasts, and two additional enzymatic steps coupled to products of PPDK catalysis (conversion of PPi to 2 Pi by pyrophosphatase and conversion of AMP + ATP to two ADP by adenylate kinase, which is supported by our previous transcriptomics study [Park et al., 2010]). Taken together, these findings demonstrate that the protocol developed is capable of isolating and separating physiologically intact chloroplasts from *B. sinuspersici*.

Intracellular Compartmentation and Function of the Two Chloroplast Types in SCC_4 Photosynthesis

The question of compartmentation in SCC_4 species, relative to Kranz-type C_4 species, was previously addressed for a few photosynthetic enzymes. Immunolocalization studies with *Bienertia* (*B. cycloptera* [Voznesenskaya et al., 2005] and *B. sinuspersici* [E.V. Voznesenskaya, N.K Koteyeva, and G.E. Edwards, unpublished data]) showed that chlorenchyma cells

in very young leaves that have just emerged have Rubisco in all chloroplasts prior to developing two cytoplasmic domains. At an intermediate stage of development, there is substantial Rubisco and PPDK in both types of chloroplasts, but with preferential labeling of Rubisco in the C-CP and PPDK in the P-CP. As chlorenchyma mature, there is strong selective labeling of Rubisco in the C-CP and selective labeling of PPDK in the P-CP, although there is some apparent labeling of PPDK in the C-CP. This suggests that P-CP and C-CP preparations from fully expanded leaves used in this study can be expected to have some PPDK in the C-CP and Rubisco in the P-CP due to a developmental gradient, in addition to any possible cross-contamination.

Majeran et al. (2005, 2008) analyzed differential protein accumulation in the MC and BSC chloroplasts of the Kranz-type C_4 plant maize by combining several large-scale proteomic approaches. They reported average BSC/MC percentage distribution for RBCL (63%–89%), RBCS (82%–87%), and PPDK (20%–40%), with average cross-contamination between the two cells types of 5% and 15%, respectively. In this study, the percentage distribution of RBCS, RBCL, and PPDK between C-CP and P-CP on a protein basis was 81%, 72%, and 20%, respectively (Fig. 2B). This indicates that in the SCC_4 species *B. sinuspersici*, the distribution of the main markers for C_4 and C_3 photosynthesis seem to be comparable to observations made in Kranz-type C_4 species and is consistent with previous immunolocalization studies. It is important to note that analysis of relative protein content by western blots is only semiquantitative and that the degree of accuracy, therefore, is limited, which may account for the differences in RBCL and RBCS, rather than in vivo differences. Since distribution by western-blot analysis was compared on a protein basis, the chloroplast preparations also needed to be free of other cellular contaminations, since this would alter the apparent protein distribution. According to our analysis, isolated chloroplasts were free of cytoplasmic, nuclear, and mitochondrial contamination and almost free of peroxisomal contamination, as seen from the absence of the respective signals for the marker enzymes PEPC, Ala-AT, cAsp-AT, mAsp-AT, NAD-ME, SHMT, GDC-P, HPR1, and histone H3 (Fig. 2B). Therefore, we conclude that the differences observed in the distribution of the marker enzymes Rubisco and PPDK, as seen in our western-blot analysis, reflect the differences between chloroplast types on a protein basis.

Based on the selective accumulation of PPDK in P-CP and RBCL in the C-CP in immunolocalization studies of *B. sinuspersici*, it was previously proposed that they function analogous to BSC and MC in Kranz-type C_4 species (Voznesenskaya et al., 2002, 2005; Chuong et al., 2006). However, the occurrence of an enzyme does not provide direct proof of a functional pathway or its capacity. Therefore, substrate-specific measurements of POE were made on intact cells, purified CC, C-CP, and P-CP, with a variety of different substrates to further understand the specific function of the two chloroplast types. Interestingly, isolated whole cells can evolve oxygen even without added HCO_3^-, probably reflecting their ability to concentrate CO_2 via the C_4 pathway (Fig. 3C). Unlike isolated cells, isolated chloroplasts were dependent on the addition of HCO_3^- to the medium, and only the C-CP and the CC were able to evolve oxygen with HCO_3^- as substrate, indicating that the operation of the C_3 cycle is limited to this chloroplast type (Table I). This was further confirmed by including the C_3 cycle inhibitor GA in the reaction medium, which abolished CO_2-dependent POE completely. GA is believed to block the C_3 cycle at the transketolase step (Stokes and Walker, 1972), indicating that illuminated C-CP continuously regenerate RuBP for the time period measured rather than using a preexisting RuBP pool. In *B. sinuspersici*, both chloroplast types show oxygen evolution with 3-PGA as a substrate. This allows cooperation between the two chloroplast types in utilizing the available reductive power. This cooperative function is analogous to Kranz-type C_4 species, in which enzymes of the reductive phase of the C_3 cycle are observed in both chloroplast types and mesophyll chloroplasts have been shown to reduce 3-PGA as part of the triose phosphate shuttle, whereas Rubisco and the enzyme that regenerates RuBP, phosphoribulokinase, are confined to BS chloroplasts (Edwards and Walker, 1983; Flugge and Heldt, 1991; Majeran and van Wijk, 2009). No 3-PGA-dependent oxygen evolution could be observed in the isolated cells, probably because 3-PGA cannot easily diffuse through the plasma membrane, which was previously observed in experiments with isolated protoplasts (Day et al., 1981).

Specialization of function in C_4 chloroplasts is not limited to the biochemistry of carbon fixation but includes specialization in the light reactions as well, to meet the energy requirements for carbon metabolism in the two compartments. In NADP-ME species such as maize, BSC chloroplasts are deficient in grana, which is correlated with increased function of PSI-dependent cyclic photophosphorylation, decreased PSII activity, and limited linear electron transport capacity (Majeran et al., 2008). Although NAD-ME C_4 species have grana in both chloroplast types, studies in different Kranz-type NAD-ME species in Chenopodiaceae show that MC chloroplasts have a reduced granal index and grana size compared with BSC (Gamalei and Voznesenskaya, 1986; Voznesenskaya and Gamalei, 1986). In the closely related and morphologically similar SCC_4 species *B. cycloptera*, the granal index of the C-CP is 1.5-fold higher and the size of the grana is significantly larger than in P-CP (Voznesenskaya et al., 2002), suggesting decreased PSII activity in P-CP. However, no evidence was found in this study for reduced capacity of PSII in the P-CP of *B. sinuspersici*, based on rates of 3-PGA-dependent oxygen evolution and oxygen evolution with the artificial Hill oxidant, pBQ. This Hill oxidant is permeable to intact chloroplasts and accepts electrons directly

from PSII, thereby providing a measure of its capacity when bypassing whole-chain electron flow (Cho et al., 1966). These results suggest that both chloroplast types in *B. sinuspersici* have a similar capacity under light-saturating conditions to produce NADPH, as well as ATP, by linear electron transport. This finding is interesting, because the proposed Asp-Ala shuttle in *B. sinuspersici* only requires ATP produced by the P-CP in order to drive the conversion of Pyr to PEP when the C_4 cycle is operating, similar to NAD-ME Kranz-type species (Edwards and Walker, 1983; Voznesenskaya et al., 1999). Besides reduction of 3-PGA, some of the reductive power generated by linear electron flow in P-CP could potentially be utilized by a chloroplastic NADP-MDH enzyme, converting OAA to MA, thereby shuttling carbon, as well as reductive power, to the CC. Mesophyll chloroplasts of some Kranz-type NAD-ME C_4 species have the capacity to reduce OAA to MA, although this capacity is lower than in NADP-ME C_4 species (Huber and Edwards, 1975). Although NADP-MDH was not previously assayed, in immunolocalization studies with an antibody from sorghum there was some labeling in both types of chloroplasts of *B. sinuspersici* (Chuong et al., 2006). However, we did not observe oxygen evolution in isolated P-CP with OAA, Pyr, or OAA and Pyr in combination. This indicates that P-CP are either impaired in OAA uptake or do not possess a functional NADP-MDH enzyme. Therefore, we directly tested for NADP-MDH activity in chloroplast extracts of P-CP and CC as well as in extracts of whole protoplasts (Fig. 4). Without prior light activation, the activity of chloroplastic NADP-MDH in vitro is dependent on the presence of a reducing agent (Johnson and Hatch, 1970), which was utilized to analyze the specificity of the reaction. There was little or no activation by DTT in extracts of CC, P-CP, or TP of *B. sinuspersici*, while there was a high level of activation of NADP-MDH by DTT in extracts from maize leaves, and there was low activity in the P-CP. In summary, the results of this study suggest that the C_4 cycle in *B. sinuspersici* is not functioning via a MA-Pyr shuttle.

Surprisingly, the highest activity of NADP-MDH in *B. sinuspersici* was found in extracts of the CC and not in P-CP. This activity may be associated with mitochondrial MDH; in the NAD-ME species *Atriplex spongiosa*, mitochondria of BS cells have NADP-MDH activity that is not activated by reducing agents (Moore et al., 1984). Recent studies with mitochondrial MDH mutants in Arabidopsis show that plant mitochondria having NADP-MDH activity are generally capable of reducing OAA to MA, and it was suggested that MA is subsequently exported to the cytosol rather than being utilized for mitochondrial respiration (Tomaz et al., 2010). Although Asp is considered the primary donor of carbon to the mitochondrial NAD-ME in *B. sinuspersici*, it is possible that some of the OAA formed by PEPC activity in the cytosol is taken up directly by the mitochondria and metabolized through NADH-MDH and ME in the CC.

Finally, in Kranz-type C_4 species, PPDK is localized in mesophyll chloroplasts, where Pyr is converted to PEP through the utilization of ATP. Previous immunolocalization studies have shown that PPDK accumulates predominantly in the P-CP of *B. cycloptera* (Voznesenskaya et al., 2005; Chuong et al., 2006). This study shows that isolated P-CP are not only enriched in PPDK; indeed, they possess a fully functional pathway for the light-driven conversion of Pyr to PEP, which indicates that they function analogous to MC chloroplasts in Kranz-type C_4 species.

Distribution of Chloroplasts between the Two Domains

The analyses showed that the P-CP are larger than the C-CP, with twice the visible surface area per chloroplast. While the P-CP have 30% more chlorophyll per chloroplast, there are approximately six times more chloroplasts in the CC; thus, the CC has approximately four times more chlorophyll than the peripheral compartment (Tables II and III; Fig. 6). In C_4 photosynthesis, there is cooperation between the two compartments and their respective chloroplast types in capturing atmospheric CO_2 and donating it to the C_3 cycle and in providing the assimilatory power needed for C_4 photosynthesis (Edwards and Walker, 1983; Edwards and Voznesenskaya, 2011). In NAD-ME-type C_4 species, the minimum energy requirement to support an Asp-Ala-type C_4 cycle is two ATP per CO_2 delivered and three ATP and two NADPH per CO_2 assimilated in the C_3 cycle. Energy production in the two chloroplast types might be correlated more to the chlorophyll content than to the relative numbers of chloroplasts. The investment of approximately four times more chlorophyll in the C-CP than in the P-CP (Table IV) suggests that chloroplasts in the CC have a greater role in providing assimilatory power to support C_4 photosynthesis. Since the two chloroplast types have similar capacity to reduce 3-PGA to triose-phosphates on a chlorophyll basis (Table I), this also indicates that the capacity for 3-PGA reduction is four times higher in the CC than in the P-CP. Interestingly, the distribution of the number of chloroplasts between the central and peripheral compartments in the SCC_4 species *B. sinuspersici* and *B. cycloptera* appears to be similar (Voznesenskaya et al., 2002). Even in *S. aralocaspica*, the other structural form of SCC_4, it was reported that the proximal chloroplasts (which functionally resemble C-CP) are more abundant than the distal chloroplasts (Voznesenskaya et al., 2001), although quantitative information was not presented in these studies. Therefore, a greater investment in the chloroplasts, which function to fix CO_2 in the C_3 cycle, appears to be a common feature of SCC_4 species. Also, in Kranz-type NAD-ME C_4 species, analyses show a higher investment in chlorophyll in the Rubisco-containing BSC chloroplasts than in the MC chloroplasts; the average for four C_4 grasses was 37% in MC and 63% in BSC (Mayne et al., 1974).

In photosynthesis in *B. sinuspersici*, considering that the primary role of the P-CP is to generate two ATP per CO_2 fixed to support an Asp-type C_4 cycle and that the primary role of the C-CP is to generate assimilatory power to support the C_3 cycle (three ATP, two NADPH), it is reasonable to suggest that more light-harvesting/photochemical capacity is needed in the CC. The exact quantum requirement in the P-CP versus C-CP per CO_2 fixed will depend on a number of factors. First, production of ATP to support the C_4 cycle through conversion of Pyr to PEP could occur by PSI-mediated cyclic electron flow or linear electron flow to oxygen or NADP based on studies with MC chloroplasts from Kranz-type C_4 species (Huber and Edwards, 1975). In terms of quantum efficiency, cyclic photophosphorylation could be the most effective means of producing ATP to support the generation of PEP. There is recent evidence for a function of PSI-mediated cyclic photophosphorylation through NDH in Arabidopsis, with NADPH as an electron donor to PSI in the cyclic pathway (Livingston et al., 2010). Also, NDH-dependent cyclic photophosphorylation is proposed to function in mesophyll chloroplasts of NAD-ME-type C_4 species (Takabayashi et al., 2005). The theoretical maximum efficiency of the NDH-dependent pathway is generation of one ATP per photon absorbed by PSI (with proton motive force of 4 H^+/e^-) via NDH and the Q cycle and utilization of approximately four H^+/ATP via ATP synthase (Steigmiller et al., 2008; Kramer and Evans, 2010). In this case, the P-CP of *B. sinuspersici* would require only two photons per two ATP synthesized per turn of the C_4 cycle. The minimum quantum requirement for the C_3 cycle per CO_2 fixed and oxygen evolved is eight, with production of two NADPH and approximately three ATP (assuming proton motive force of 12 H^+, with use of four H^+ per ATP produced). Obviously, more quanta need to be absorbed and utilized by chloroplasts in the CC, since this is the primary site for providing energy to support the C_3 cycle. Beyond these calculated minimum requirements, in practice, the energy requirements per net CO_2 fixed by the C_3 cycle are expected to be somewhat higher in both types of chloroplasts. In addition to providing ATP to support PPDK activity, the quantum requirement in the P-CP will be higher to the extent that there is overcycling of the C_4 pathway and leakage of CO_2 from the CC and to the extent that there is movement of some 3-PGA from the C-CP to the P-CP for reduction. The capacity of the P-CP to reduce 3-PGA provides flexibility in utilizing the energy produced by the two chloroplast types to meet the needs for carbon assimilation. In the C-CP, the energy requirements per net CO_2 fixed by Rubisco will be higher to the extent that photorespiration is occurring. It is also possible that the C-CP are less efficient than the P-CP in the absorption of solar energy, due to the tight packing of the chloroplasts in the CC.

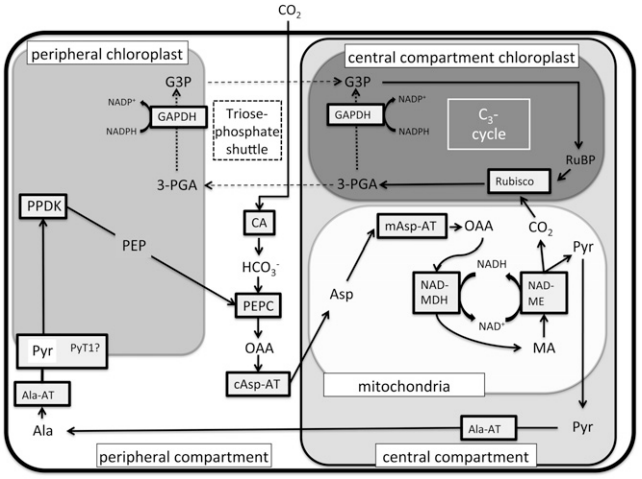

Figure 7. Model for CO_2 fixation in *B. sinuspersici*. Explanation is found in the text. G3P, Glyceraldehyde-3-phosphate; GAPDH, G3P phosphate dehydrogenase.

Model for the C_4 Pathway in *B. sinuspersici*

The results of this study support the following scheme for photosynthesis in the SCC_4 species *B. sinuspersici* (Fig. 7). Atmospheric CO_2 enters the photosynthetic cell, where cytosolic CA converts it to bicarbonate, which is then utilized as the source of inorganic carbon for cytosolic PEPC. The primary carbon acceptor, PEP, which is required to form OAA, is produced by the P-CP. An Asp-Ala shuttle is proposed, as we found no evidence for OAA being converted to MA by the P-CP. Additionally, we observed localization of Ala-AT and c-Asp-AT to the cytoplasm and mAsp-AT to the mitochondria, and these enzymes increase during development of the C_4 system in *B. sinuspersici* (Lara et al., 2008), which provides further evidence for the proposed pathway. Furthermore, Park et al. (2010) recently found evidence for the occurrence of all 10 enzymes required to support an Asp-Ala C_4 cycle shuttle in *B. sinuspersici* in a proteomics study. Therefore, OAA is likely converted by cAsp-AT to Asp, which is then imported into the mitochondria of the CC. Within the mitochondria, Asp is transaminated back to OAA, reduced to MA by NAD-MDH, and decarboxylated by NAD-ME. All the mitochondria of the cell are located in the central compartment, and immunolocalization studies show that NAD-ME is located in the mitochondria (Voznesenskaya et al., 2002; Chuong et al., 2006), which supports the scheme. The released CO_2 diffuses into the surrounding C-CP, where it is finally fixed by Rubisco of the C_3 cycle. The reduction of 3-PGA to glyceraldehyde-3-phosphate is proposed to occur largely in the C-CP, with supplemental reduction by P-CP via a triose-phosphate shuttle (dashed lines). Finally, Pyr from the decarboxylation of MA is exported from the mitochondria, transaminated to Ala, which diffuses to the peripheral cytoplasm, where it is

converted to Pyr. The Pyr is then imported back into the P-CP, presumably by the putative Pyr transporter PyT1. Besides having the decarboxylation phase of the C_4 cycle and the C_3 cycle in the CC, this is also the site of any photorespiration that will occur, via the chloroplasts, mitochondria, and peroxisomes, due to some oxygen reacting with RuBP in the C-CP. Markers for GDC-P and SHMT appear in the CC, which could support mitochondrial conversion of two Gly to Ser + CO_2 + NH_3 through the glycolate pathway. Immunolocalization studies demonstrate localization of the GDC-P peptide in the mitochondria of the CC in *B. cycloptera* (Voznesenskaya et al., 2002). The occurrence of HPR in the CC could support a terminal step in the glycolate pathway through the reduction of hydroxypyruvate to glycerate in the peroxisomes.

SUMMARY AND CONCLUSION

C_4 photosynthesis requires the spatial separation of initial CO_2 fixation by an oxygen-insensitive carboxylase, PEPC, and final CO_2 fixation by Rubisco of the C_3 cycle. This can be implemented by either having two chloroplast types localized in different tissues, as in Kranz-type C_4, or in having two functional domains within a cell, as in SCC_4. In both cases, the effective CO_2 concentration available for Rubisco is increased, thereby minimizing its oxygenase activity and, consequently, photorespiration in C_4 plants. This work and previous studies all indicate that the two SCC_4 *Bienertia* species function very similar to Kranz-type C_4 species, including the development of a C_4-type PEPC, development of separate domains for spatial separation of functions and physiological responses typical of C_4 plants, and performance of C_4 in natural habitats based on carbon isotope values of biomass (Edwards et al., 2004; Akhani et al., 2005, 2009; Lara et al., 2006; Smith et al., 2009; Leisner et al., 2010).

Finally, as demonstrated in this study, the biochemistry and the functionality of the chloroplasts in *B. sinuspersici* are similar to related NAD-ME Kranz-type C_4 species. Chloroplasts of Kranz-type C_4 species have been shown to differentially accumulate large sets of proteins in the two involved chloroplast types, and there is considerable evidence for transcriptional control between MC and BSC (Hibberd and Covshoff, 2010). *B. sinuspersici* is an important system for future study, since its chloroplast differentiation is analogous to Kranz-type C_4 species, although control cannot occur at the transcriptional level. Therefore, alternative mechanisms, such as selective protein import or differential mRNA targeting to the two cytoplasmic domains, may be crucial for the development and function of dimorphic chloroplasts. Our chloroplast isolation protocol will allow in-depth study of these two chloroplast types. This includes studies on the protein composition of the dimorphic chloroplasts and protein import assays to determine if chloroplast differentiation is controlled by selective import of nucleus-encoded proteins.

MATERIALS AND METHODS

Plant Material and Growth Conditions

Bienertia sinuspersici was propagated from cuttings and grown in computer-controlled growth chambers (Econair GC-16; Bio Chambers) at a maximum of 1,000 PPFD, a 14/10-h light/dark photoperiod, a 35°C/18°C day/night temperature regime, atmospheric CO_2, and 50% relative humidity. Plants were grown in commercial potting soil in 7-gallon pots (one plant per pot) and watered once a week with 1 g L^{-1} Peters Professional fertilizer (20:20:20) and a 150 mM NaCl solution. The lights in the chamber were programmed to come on and off gradually through a stepwise increase or decrease over a 2-h period at the beginning and end of the photoperiod, respectively. Mature leaves from 3- to 9-month-old plants were used for this study.

Chloroplast Isolation

Throughout the chloroplast isolation procedure, we refer to "washing" as a cycle of pelleting and resuspending in the indicated buffers and for the given conditions. For photosynthetic measurements, plant material was harvested in the morning before the onset of illumination to keep chloroplast starch levels low. Leaf osmolality of plant material to be used was determined prior to each experiment with a 5500 Vapor Pressure Osmometer (Wescor), and then 150 mature leaves were harvested. Internal solute concentrations in *B. sinuspersici* cells varied significantly (1,000–1,800 mosmol kg^{-1}) depending on age, salt treatment, and watering status of the plant. Therefore, Gly betaine was added to all buffers for the cell, protoplast, and chloroplast isolations at a level (1–1.8 M) to match internal levels of solutes for each experiment (the required concentrations are referred to as matching Gly betaine concentrations hereafter). All steps to obtain protoplasts were carried out at room temperature unless otherwise indicated. Chlorenchyma cells were isolated by gently squeezing leaves for 5 min with a pestle in a ceramic mortar in 15 mL of protoplast buffer (5 mM MES-NaOH, pH 5.8, 10 mM $CaCl_2$, and matching Gly betaine concentration). The solution was filtered through a nylon mesh with 1-mm pore size to remove the epidermis. Cells were washed twice in 15 mL of protoplast buffer (5 min, 3.5*g* in a Damon IEC HN-SII centrifuge) and resuspended in 6 mL of protoplast buffer. Aliquots were taken for analysis of TC, and intactness was assessed with light microscopy by mixing 5 μL of isolated cells with 5 μL of 10% (w/v) trypan blue dye. Cells were distributed into three 2-mL round-bottom centrifuge tubes, with the following steps being carried out in parallel in these three tubes. Cells were pelleted for 5 min at 9*g* in a benchtop centrifuge and resuspended in 1 mL of digestion buffer (5 mM MES-NaOH, pH 5.8, 10 mM $CaCl_2$, 2% [w/v] Sumizyme C [Shin-Nihon Chemical], 0.25% [w/v] Macerase [Calbiochem], and matching Gly betaine concentration). Cells were incubated for 1 h at 35°C on a Gyromax 737 orbital incubator shaker (Amerex Instruments) at 65 rpm with illumination from a 100-W light bulb to obtain protoplasts. All of the following steps were carried out at 4°C. Protoplasts were washed twice (5 min, 15*g* using a benchtop centrifuge) in 2 mL of protoplast buffer and once in 2 mL of protoplast resuspension buffer (20 mM Tricine-KOH, pH 8.4, 10 mM EDTA, 10 mM $NaHCO_3$, and matching Gly betaine concentration). An aliquot was removed for analysis of total protoplasts and kept on ice until used. Protoplasts were resuspended in 500 μL of protoplast lysis buffer (PLB; 20 mM Tricine-KOH, pH 8.4, 10 mM EDTA, 10 mM $NaHCO_3$, 1% [w/v] bovine serum albumin, and matching Gly betaine concentration). Protoplasts were then disrupted by stepwise reduction of the buffer osmolality. Next, 200 μL of PLB without Gly betaine was added and mixed immediately by inverting the tube. Protoplasts were incubated for 60 s on ice, and the procedure was repeated by again adding 200 μL of PLB without Gly betaine. Protoplasts were transferred to a 10-cm × 1-cm glass reagent tube, and the tube was closed with a rubber stopper. The tube was quickly inverted six times to disrupt the protoplasts, and aliquots were analyzed with a microscope. The procedure was repeated until most protoplasts (more than 90%) were broken. Following this, 3 mL of PLB without bovine serum albumin was added, and the solution was centrifuged for 5 min at 40*g* (Sorvall RC5C centrifuge, equipped with an HB4 swinging-bucket rotor) to separate P-CP from CC. The supernatant containing P-CP was transferred to a new glass tube and centrifuged two more

times at 40*g* to remove the remaining CC. The P-CP were kept on ice until the final Percoll purification step. The pellet enriched in CC was resuspended in 6 mL of PLB and filtered through a 30-μm nylon mesh to remove any remaining intact protoplasts and cellular debris. CC were pelleted (5 min, 20*g*) and resuspended in 3 mL of PLB. A 500-μL aliquot was removed, mixed with 2.5 mL of PLB, pelleted again, resuspended in 3 mL of PLB, and stored on ice until the final Percoll purification. The remaining CC were pelleted (5 min, 20*g*), resuspended in 800 μL of CC breaking buffer (50 mM Tris-HCl, pH 9.5, 5 mM $MgCl_2$, 2.5 mM EDTA, and Gly betaine to match the organelle osmolality), and incubated for 15 min on ice. Chloroplasts were released from CC by pipetting eight times up and down with a 200-μL Gilson-type pipette tip on top of a 1,000-μL tip. Aliquots were analyzed with a light microscope, and the procedure was repeated until most (more than 70%) of the CC were disrupted. Next, 3 mL of PLB was added and the remaining intact CC were pelleted (5 min, 40 *g*). The supernatant containing C-CP was transferred to a new glass tube and centrifuged again (5 min, 40*g*). The fractions of isolated P-CP, C-CP, and CC (each in 3 mL of PLB) were finally added on top of a two-step Percoll cushion. The lower cushion consisted of 2 mL of 80% (v/v) Percoll, 20 mM HEPES-KOH, pH 7.6, 5 mM $MgCl_2$, and 2.5 mM EDTA. The lower cushion was overlaid with medium containing 5 mL of 40% (v/v) Percoll, 1.2% (w/v) polyethylene glycol 6000, 0.4% (w/v) Ficoll, 20 mM HEPES-KOH, pH 7.6, 5 mM $MgCl_2$, and 2.5 mM EDTA. Each cushion contained Gly betaine at a concentration matching the osmolality of the cell preparations. The tubes were centrifuged for 6 min at 2,500*g* in a Sorvall RC5C centrifuge equipped with an HB4 swinging-bucket rotor. The supernatant containing the band of broken chloroplasts was discarded, and the lower green band at the 40%-80% Percoll interface was carefully removed. For protein analysis, a one-step Percoll cushion without the 80% Percoll solution was used, and the intact chloroplast pellet was frozen until further use at −20°C.

Protein Extraction and Western-Blot Analysis

Total protein extracts from isolated fractions were prepared by resuspending the pellets in 200 μL of extraction buffer (2% [w/v] SDS, 10% [w/v] glycerol, 62.5 mM Tris-HCl, pH 6.8, and 0.715 M 2-mercaptoethanol) and boiled for 5 min. Insoluble material was removed by centrifugation (10 min, 16,000*g*) in a benchtop centrifuge. Protein concentration was determined with an RCDC protein quantification kit (Bio-Rad), which tolerates detergents and reducing agents. SDS-PAGE was performed on 10% (w/v) or 15% (w/v) polyacrylamide gels according to Laemmli (1970). To guard against overloading, which was based on initial staining patterns with the dilutions of antibodies selected, 5 μg of protein was added per lane for RBCL, RBCS, PEPC, and PPDK and 20 μg of protein was added per lane for other proteins. Proteins were electroblotted onto nitrocellulose membranes for immunoblotting according to Burnette (1981). Bound antibodies were located by linking to alkaline phosphatase-conjugated goat anti-rabbit IgG. The antibodies used for detection, with dilutions in parentheses, were as follows: anti-*Nicotiana tabacum* Rubisco large subunit (1:10,000; courtesy of Dr. R. Chollet); anti-*Amaranthus hypochondriacus* Rubisco small subunit (1:10,000; courtesy of Dr. J. Berry); anti-*Zea mays* PPDK (1:50,000; courtesy of Dr. C. Chastain); anti-*Spinacia oleracea* choline monoxygenase (1:1,000; courtesy of Dr. A.D. Hanson); anti-β-subunit of ATP synthase (CF1-β; 1:10,000; courtesy of Dr. A. Barkan); anti-*Flaveria bidentis* PyT1 (1:10,000; courtesy of Dr. T. Furumoto); anti-*Amaranthus viridis* PEPC (1:100,000; Colombo et al., 1998); anti-histone H3 (1:5,000; Abcam ab1791); serum against the α-subunit of NAD-ME from *A. hypochondriacus* (1:2,000; Long et al., 1994); anti-SHMT (1:10,000; courtesy of Dr. H. Bauwe); anti-GDC-P (1:10,000; courtesy of Dr. D. Oliver); anti-*S. oleracea* peroxisomal HPR1 (1:10,000; courtesy of Dr. H. Bauwe; Timm et al., 2008); anti-*Panicum miliaceum* Ala-AT (1:10,000; specific for C_4 isoform-Ala-AT-2 in the NAD-ME C_4 species *P. miliaceum*; Son et al., 1991); cAsp-AT (1:10,000; courtesy of Dr. M. Taniguchi; Sentoku et al., 2000); and anti-*Eleusine coracana* mAsp-AT (1:10,000; specific for the mitochondrial isoform in the NAD-ME species *E. coracana*; Taniguchi and Sugiyama, 1990). The molecular masses of the polypeptides were estimated from a plot of the log of the molecular masses of marker standards versus migration distance. The intensities of bands on western blots were semiquantified with ImageJ image-analysis software (Abramoff et al., 2004) and expressed relative to levels in total protoplasts.

CA Activity

CA activity was determined essentially as described by Wilbur and Anderson (1948) and Worthington (1988) with the following modifications. Protoplasts from 100 mature *Bienertia* leaves were isolated as described previously and resuspended in 3 mL of 20 mM Tris-sulfate buffer (pH 8.3 at 25°C) and matching Gly betaine concentration as described earlier. Aliquots (200 μL) of protoplasts were diluted in 1.8 mL of Tris-sulfate buffer, and protoplasts were disrupted by pipetting gently up and down with a 200-μL Gilson-type pipette tip. Complete rupture of protoplasts was monitored with a light microscope.

CA activity was assayed either in total protoplast extracts or in chloroplast pellets and supernatant fractions following disruption of protoplasts and centrifugation for 2.5 min at 1,500*g*. The chloroplast-containing pellet was resuspended again in 2 mL of Tris-sulfate buffer and centrifuged again under the same conditions. The pellet was finally resuspended in 2 mL of Tris-sulfate buffer. The protoplast extract, the resuspended chloroplast pellet, and the supernatant were sonicated (eight pulses, 50% power) with a model 300 V/T ultrasonicator equipped with a microtip horn (Biologics). A 200-μl aliquot was removed for analysis of chloroplast integrity by monitoring soluble stromal proteins RBCL and PPDK by western-blot analysis, and the remaining 1.8 mL was used for analysis of CA. Activity was measured titermetrically by adding 1 mL of CO_2-saturated water, and the time required for the pH to change from 8.3 to 6.3 was recorded. All equipment and buffers were prechilled to 0°C. Wilbur-Anderson units were calculated as follows: $(time_b - time_s)/time_s$, where b = blank and s = sample, with time given in seconds and rates expressed as units mg^{-1} total protein in the protoplast extract.

Photosynthetic Oxygen Evolution

For measurement of POE, isolated fractions were mixed 1:1 with double-strength chloroplast storage buffer (20 mM KCl, 2 mM EDTA, 2 mM $MgCl_2$, 2 mM $MnCl_2$, 2% [w/v] bovine serum albumin, 10 mM HEPES-KOH, pH 7.6, 10 mM $Na_4P_2O_7$, 0.4 mM K_2HPO_4, 2 mM ATP, and matching Gly betaine concentration). While none of the components (except the osmoticum Gly betaine) were essential for oxygen evolution, it was noted that isolated chloroplasts degraded rather quickly (about 50% loss of activity by storage for 2 h on ice). Storage in this complex buffer improved chloroplast stability significantly (greater than 90% of the original activity after 6 h of storage on ice). POE measurements were performed on a chlorophyll basis. Chlorophyll was extracted in 80% (v/v) acetone. Since the treatment did not efficiently extract chlorophyll from TC, ultrasonication was used to disrupt the cell walls (four times four pulses, 50% power with a model 300 V/T ultrasonicator [Biologics] equipped with a microtip horn). Samples were cooled on ice for 5 min in the dark between the cycles. To ensure comparability between the different fractions, the same treatment was also applied to isolated chloroplasts. Insoluble material was removed by centrifugation (10 min, 16,000*g* with a benchtop centrifuge), and chlorophyll concentration was determined as described by Arnon (1949). Equal amounts of the different fractions, corresponding to 12.5 μg of total chlorophyll, were resuspended in 500 μL of POE buffer (10 mM KCl, 1 mM EDTA, 50 mM HEPES-KOH, pH 7.6, 1 mM ATP, 5 mM $Na_4P_2O_7$, 0.2 mM K_2HPO_4, 200 units of catalase, and matching Gly betaine concentration). Substrate-specific POE (Fig. 3; Table I) was measured by adding one of the following substrates: 10 mM $NaHCO_3$, 5 mM 3-PGA, 2.5 mM ferricyanide + 5 mM NH_4Cl_2, 125 μM pBQ, 10 mM GA, 10 mM Pyr, or 2 mM OAA. Measurements were performed using a Rank Brothers oxygen electrode. The reaction mixture of 500 μL was illuminated with an incandescent lamp giving a light intensity at the surface of the cuvette of 1,000 μmol quanta $m^{-2}\,s^{-1}$ (except for Fig. 3A, where light intensities are indicated in the figure). All measurements were performed at 25°C (except for Fig. 3B, where the temperatures are indicated in the figure). POE in all measurements was monitored for at least 10 min.

NADP-MDH Assay

NADP-MDH was assayed as described previously (Kanai and Edwards, 1973). In brief, isolated CC, P-CP, and TP and whole maize leaf extracts corresponding to 10 μg of total chlorophyll were incubated for 15 min at room temperature in a buffer containing 50 mM Tricine-KOH, pH 8, in the presence or absence of 25 mM DTT. Maize enzyme extracts were prepared by grinding whole leaves in a buffer containing 50 mM Tricine-KOH, pH 8, 5 mM $MgCl_2$, and 5 mM DTT. The homogenate was filtered through a 30-μm nylon net, and the filtrate was taken as the enzyme preparation. Then, 0.2 mM NADPH was added to the reaction mixture, and the spectrophotometer was blanked. The reaction was initiated by adding 3 mM OAA, and NADP-MDH was assayed spectrophotometrically by monitoring the oxidation of NADPH at 340 nm and 35°C.

Pyr-to-PEP Conversion by Chloroplasts

For analysis of PEP formation, isolated chloroplasts were resuspended after Percoll purification in double-strength chloroplast isolation buffer without ATP. Material corresponding to 20 μg of total chlorophyll was then diluted in PEP buffer I (50 mM HEPES-KOH, pH 7.6, 0.2 mM K_2HPO_4, 1 mM NaCl, 5 mM KCl, 1 mM EDTA, 3 mM Pyr, and matching Gly betaine concentration) in a total volume of 1 mL. Chloroplasts were illuminated for the times indicated in Figure 5, with 1,000 μmol quanta m^{-2} s^{-1} at 25°C in a Rank Brothers oxygen electrode chamber under constant stirring. Chloroplasts were pelleted (2 min, 16,000*g* with a benchtop centrifuge), and 100 μL of the supernatant was mixed with 500 μL of PEP buffer II (100 mM HEPES-KOH, pH 7.6, 15 mM $MgCl_2$, 0.15 mM EDTA, 5 mM $NaHCO_3$, 0.3 mM NADH, 5 mM NH_4Cl, 2.5 mM K_2HPO_4, 5 mM DTT, 1 mM Glc-6-P, and 1.5 mM ATP). The spectrophotometer was blanked, and the reaction was initiated by adding 10 units of MDH (Sigma) and 3 units of PEPC (MP Biomedicals). Oxidation of NADH was monitored spectrophotometrically at 340 nm and 35°C. Standard curves were prepared with PEP.

Chloroplast Count, and Chlorophyll and Protein Determination

Chlorophyll and total protein contents were determined from Percoll-purified chloroplasts. Chlorophyll was extracted in 80% (v/v) acetone, and the precipitated protein pellet from this preparation was boiled in 1× SDS loading buffer without bromphenol blue and used to determine total protein concentration with Bio-Rad's RCDC protein quantification kit. Particles in diluted aliquots of each preparation were counted in a hematocytometer to allow the calculation of chlorophyll and protein per chloroplast or cell. For determination of the number of P-CP and C-CP per cell, isolated protoplasts were gently squeezed between the glass slide and the coverslip and observed with a light microscope. Photographs were taken, and the individual chloroplasts were marked with the aid of image-manipulation software to avoid redundant counting.

ACKNOWLEDGMENTS

We thank R.M. Sharpe and C.P. Leisner for critical reading of the manuscript and C. Cody for plant growth management.

Received December 1, 2010; accepted January 15, 2011; published January 24, 2011.

LITERATURE CITED

Abramoff M, Magelhaes P, Ram S (2004) Image processing with ImageJ. Biophotonics International **11:** 36–42

Akhani H, Barroca J, Koteeva N, Voznesenskaya E, Franceschi V, Edwards G, Ghaffari SM, Ziegler H (2005) *Bienertia sinuspersici* (Chenopodiaceae): a new species from southwest Asia and discovery of a third terrestrial C_4 plant without Kranz anatomy. Syst Bot **30:** 290–301

Akhani H, Lara MV, Ghasemkhani M, Ziegler H, Edwards GE (2009) Does *Bienertia cycloptera* with the single-cell system of $C(_4)$ photosynthesis exhibit a seasonal pattern of delta $^{(13)}C$ values in nature similar to co-existing $C(_4)$ Chenopodiaceae having the dual-cell (Kranz) system? Photosynth Res **99:** 23–36

Arnon DI (1949) Copper enzymes in isolated chloroplasts: polyphenoloxidase in *Beta vulgaris*. Plant Physiol **24:** 1–15

Burnette WN (1981) "Western blotting": electrophoretic transfer of proteins from sodium dodecyl sulfate-polyacrylamide gels to unmodified nitrocellulose and radiographic detection with antibody and radioiodinated protein A. Anal Biochem **112:** 195–203

Cho DH, Parks L, Zweig G (1966) Photoreduction of quinones by isolated spinach chloroplasts. Biochim Biophys Acta **126:** 200–206

Chuong SD, Franceschi VR, Edwards GE (2006) The cytoskeleton maintains organelle partitioning required for single-cell C_4 photosynthesis in Chenopodiaceae species. Plant Cell **18:** 2207–2223

Colombo SL, Andreo CS, Chollet R (1998) The interaction of shikimic acid and protein phosphorylation with PEP carboxylase from the C_4 dicot Amaranthus viridis. Phytochemistry **48:** 55–59

Day DA, Jenkins CLD, Hatch MD (1981) Isolation and properties of functional mesophyll protoplasts and chloroplasts from *Zea mays*. Aust J Plant Physiol **8:** 21–29

Edwards G, Walker DA (1983) C_3, C_4: Mechanisms, and Cellular and Environmental Regulation, of Photosynthesis. University of California Press, Berkeley

Edwards GE, Franceschi VR, Ku MS, Voznesenskaya EV, Pyankov VI, Andreo CS (2001) Compartmentation of photosynthesis in cells and tissues of $C(_4)$ plants. J Exp Bot **52:** 577–590

Edwards GE, Franceschi VR, Voznesenskaya EV (2004) Single-cell $C(_4)$ photosynthesis versus the dual-cell (Kranz) paradigm. Annu Rev Plant Biol **55:** 173–196

Edwards GE, Voznesenskaya EV (2011) C_4 photosynthesis: Kranz forms and single-cell C_4 in terrestrial plants. *In* AS Raghavendra, RF Sage, eds, C_4 Photosynthesis and Related CO_2 Concentrating Mechanisms, Vol 32. Springer, Dordrecht, The Netherlands, pp 29–61

Flugge UI, Heldt HW (1991) Metabolite translocators of the chloroplast envelope. Annu Rev Plant Physiol Plant Mol Biol **42:** 129–144

Furomoto T, Yamaguchi T, Ichie Y, Takahashi Y, Izui K (2009) Identification of a plastid Na^+ dependent pyruvate transporter in plants. Poster 38, Membrane biology and transport. *In* Plant Biology 2009, July 18–July 22, Honolulu, HI. American Society of Plant Biologists, Rockville, MD, no. P38026

Galella G, Smith DB (1979) Stability of microtubule protein over the pH range: 6.9-9.5. Can J Biochem **57:** 1368–1375

Gamalei YV, Voznesenskaya EV (1986) Structural-biochemical types of C_4 plants. Sov Plant Physiol **33:** 616–630

Hatch MD (1987) C_4 photosynthesis: a unique blend of modified biochemistry, anatomy and ultrastructure. Biochim Biophys Acta **895:** 81–106

Hatch MD, Osmond CB (1976) Compartmentation and transport in C_4 photosynthesis. *In* CR Stocking, U Heber, eds, Encyclopedia of Plant Physiology, New Series, Vol 3. Springer-Verlag, Berlin, pp 144–184

Hibberd JM, Covshoff S (2010) The regulation of gene expression required for C_4 photosynthesis. Annu Rev Plant Biol **61:** 181–207

Huber SC, Edwards GE (1975) Regulation of oxaloacetate, aspartate, and malate formation in mesophyll protoplast extracts of three types of $C(_4)$ plants. Plant Physiol **56:** 324–331

Johnson HS, Hatch MD (1970) Properties and regulation of leaf nicotinamide-adenine dinucleotide phosphate-malate dehydrogenase and 'malic' enzyme in plants with the C_4-dicarboxylic acid pathway of photosynthesis. Biochem J **119:** 273–280

Kanai R, Edwards GE (1973) Separation of mesophyll protoplasts and bundle sheath cells from maize leaves for photosynthetic studies. Plant Physiol **51:** 1133–1137

Kramer DR, Evans JR (2011) Update. The importance of energy balance in improving photosynthetic productivity. Plant Physiol **155:** 70–78

Laemmli UK (1970) Cleavage of structural proteins during the assembly of the head of bacteriophage T4. Nature **227:** 680–685

Lara MV, Chuong SDX, Akhani H, Andreo CS, Edwards GE (2006) Species having C_4 single-cell-type photosynthesis in the Chenopodiaceae family evolved a photosynthetic phosphoenolpyruvate carboxylase like that of Kranz-type C_4 species. Plant Physiol **142:** 673–684

Lara MV, Offermann S, Smith M, Okita TW, Andreo CS, Edwards GE (2008) Leaf development in the single-cell C_4 system in *Bienertia sinuspersici*: expression of genes and peptide levels for C_4 metabolism in relation to chlorenchyma structure under different light conditions. Plant Physiol **148:** 593–610

Leisner CP, Cousins AB, Offermann S, Okita TW, Edwards GE (2010) The effects of salinity on photosynthesis and growth of the single-cell C_4 species *Bienertia sinuspersici* (Chenopodiaceae). Photosynth Res **106:** 201–214

Lilley RM, Fitzgerald MP, Rienits KG, Walker DA (1975) Criteria of intactness and the photosynthetic activity of spinach chloroplast preparations. New Phytol **75:** 1–10

Livingston AK, Cruz JA, Kohzuma K, Dhingra A, Kramer DM (2010) An *Arabidopsis* mutant with high cyclic electron flow around photosystem I (hcef) involving the NADPH dehydrogenase complex. Plant Cell **22:** 221–233

Long JJ, Wang JL, Berry JO (1994) Cloning and analysis of the C_4 photosynthetic NAD-dependent malic enzyme of amaranth mitochondria. The J Biol Chem **269:** 2827–2833

Majeran W, Cai Y, Sun Q, van Wijk KJ (2005) Functional differentiation of bundle sheath and mesophyll maize chloroplasts determined by comparative proteomics. Plant Cell **17:** 3111–3140

Majeran W, van Wijk KJ (2009) Cell-type-specific differentiation of chloroplasts in C_4 plants. Trends Plant Sci **14:** 100–109

Majeran W, Zybailov B, Ytterberg AJ, Dunsmore J, Sun Q, van Wijk KJ (2008) Consequences of C_4 differentiation for chloroplast membrane proteomes in maize mesophyll and bundle sheath cells. Mol Cell Proteomics **7:** 1609–1638

Mayne BC, Dee AM, Edwards GE (1974) Photosynthesis in mesophyll protoplasts and bundle sheath cells of various type of C_4 plants. III. Fluorescence emission spectra, delayed light emission, and P700 content. Z Pflanzenphysiol **74:** 275–291

Moore BD, Ku MSB, Edwards GE (1984) Isolation of leaf bundle sheath protoplasts from C_4 dicot species and intracellular-localization of selected enzymes. Plant Sci Lett **35:** 127–138

Ogren WL (1984) Photorespiration: pathways, regulation, and modification. Annu Rev Plant Physiol Plant Mol Biol **35:** 415–442

Oikawa K, Kasahara M, Kiyosue T, Kagawa T, Suetsugu N, Takahashi F, Kanegae T, Niwa Y, Kadota A, Wada M (2003) Chloroplast unusual positioning1 is essential for proper chloroplast positioning. Plant Cell **15:** 2805–2815

Park J, Knoblauch M, Okita TW, Edwards GE (2009) Structural changes in the vacuole and cytoskeleton are key to development of the two cytoplasmic domains supporting single-cell $C(_4)$ photosynthesis in *Bienertia sinuspersici*. Planta **229:** 369–382

Park J, Okita TW, Edwards GE (2010) Expression profiling and proteomic analysis of isolated photosynthetic cells of the non-Kranz C_4 species *Bienertia sinuspersici*. Funct Plant Biol **37:** 1–13

Sage RF (2004) The evolution of C_4 photosynthesis. New Phytol **161:** 341–370

Sentoku N, Taniguchi M, Sugiyama T, Ishimaru K, Ohsugi R, Takaiwa F, Toki S (2000) Analysis of the transgenic tobacco plants expressing *Panicum miliaceum* aspartate aminotransferase genes. Plant Cell Rep **19:** 598–603

Smith ME, Koteyeva NK, Voznesenskaya EV, Okita TW, Edwards GE (2009) Photosynthetic features of non-Kranz type C_4 versus Kranz type C_4 and C_3 species in subfamily Suaedoideae (Chenopodiaceae). Funct Plant Biol **36:** 770–782

Son D, Jo J, Sugiyama T (1991) Purification and characterization of alanine aminotransferase from *Panicum miliaceum* leaves. Arch Biochem Biophys **289:** 262–266

Steigmiller S, Turina P, Gräber P (2008) The thermodynamic H^+/ATP ratios of the H^+-ATPsynthases from chloroplasts and *Escherichia coli*. Proc Natl Acad Sci USA **105:** 3745–3750

Stokes DM, Walker DA (1972) Photosynthesis by isolated chloroplasts: inhibition by DL-glyceraldehyde of carbon dioxide assimilation. Biochem J **128:** 1147–1157

Takabayashi A, Kishine M, Asada K, Endo T, Sato F (2005) Differential use of two cyclic electron flows around photosystem I for driving CO_2-concentration mechanism in C_4 photosynthesis. Proc Natl Acad Sci USA **102:** 16898–16903

Taniguchi M, Sugiyama T (1990) Aspartate aminotransferase from *Eleusine coracana*, a C_4 plant: purification, characterization, and preparation of antibody. Arch Biochem Biophys **282:** 427–432

Timm S, Nunes-Nesi A, Pärnik T, Morgenthal K, Wienkoop S, Keerberg O, Weckwerth W, Kleczkowski LA, Fernie AR, Bauwe H (2008) A cytosolic pathway for the conversion of hydroxypyruvate to glycerate during photorespiration in *Arabidopsis*. Plant Cell **20:** 2848–2859

Tomaz T, Bagard M, Pracharoenwattana I, Lindén P, Lee CP, Carroll AJ, Ströher E, Smith SM, Gardeström P, Millar AH (2010) Mitochondrial malate dehydrogenase lowers leaf respiration and alters photorespiration and plant growth in Arabidopsis. Plant Physiol **154:** 1143–1157

von Caemmerer S, Furbank RT (2003) The $C(_4)$ pathway: an efficient $CO(_2)$ pump. Photosynth Res **77:** 191–207

Voznesenskaya EV, Franceschi VR, Kiirats O, Artyusheva EG, Freitag H, Edwards GE (2002) Proof of C_4 photosynthesis without Kranz anatomy in *Bienertia cycloptera* (Chenopodiaceae). Plant J **31:** 649–662

Voznesenskaya EV, Franceschi VR, Kiirats O, Freitag H, Edwards GE (2001) Kranz anatomy is not essential for terrestrial C_4 plant photosynthesis. Nature **414:** 543–546

Voznesenskaya EV, Franceschi VR, Pyankov VI, Edwards GE (1999) Anatomy, chloroplast structure and compartmentation of enzymes relative to photosynthetic mechanisms in leaves and cotyledons of species in the tribe Salsoleae (Chenopodiaceae). J Exp Bot **50:** 1779–1795

Voznesenskaya EV, Gamalei YV (1986) The ultrastructural characteristics of leaf types with Kranz anatomy. Bot Z **71:** 1291–1307

Voznesenskaya EV, Koteyeva NK, Chuong SDX, Akhani H, Edwards GE, Franceschi VR (2005) Differentiation of cellular and biochemical features of the single-cell C_4 syndrome during leaf development in *Bienertia cycloptera* (Chenopodiaceae). Am J Bot **92:** 1784–1795

Wilbur KM, Anderson NG (1948) Electrometric and colorimetric determination of carbonic anhydrase. J Biol Chem **176:** 147–154

Worthington (1988) Worthington Enzyme Manual. Worthington Biochemical, Freehold, NJ, pp 57–59